

NASA CR-
151706

SPACE SCIENCES LABORATORY

APOLLO-SOYUZ TEST PROJECT

Emb

FINAL REPORT

HELIUM GLOW DETECTOR EXPERIMENT
MA-088

(NASA-CR-151706) HELIUM GLOW DETECTOR EXPERIMENT, MA-088 Final Report (California Univ.) 103 p HC A06/DF A01 CSCI 03B N78-22991

Unclass
G3/90 16647

NASA Contract NAS9-13799



UNIVERSITY OF CALIFORNIA, BERKELEY

Combined w/ 9-13807

UCBSSL Series 18, Issue 76.

APOLLO-SOYUZ TEST PROJECT

FINAL REPORT

HELIUM GLOW DETECTOR EXPERIMENT
MA-088

NASA Contract NAS9-13799

Submitted by:

Prof. C. Stuart Bowyer
Space Sciences Laboratory
University of California
Berkeley, California 94720

15 January 1978

TABLE OF CONTENTS

1.	The MA-088 HGD Data	Page 1
2.	Applications of the HGD Data	2
2.1	The nighttime HeI 584 Å emission	2
2.2	The daytime HeI 584 Å emission	10
3.	A Hot Model of the Interstellar Medium	12
4.	References	17
5.	Figures	19
6.	Appendixes	23
6.1	Observations of Interstellar Helium with a Gas Absorption Cell: Implications for the Structure of the Local ISM	
6.2	Extreme Ultraviolet Dayglow Observations with a Helium Gas Absorption Cell.	
6.3	EUV Scattering from Local Interstellar Helium at Nonzero Temperatures: Implications for the Derivations of ISM Parameters	

1. THE MA-088 HGD DATA

Of the two 584 Å channels in the MA-088, namely #1 and #3, channel #1 appeared to provide data with erratic count rates and undue susceptibility to dayglow and solar contamination possibly because of filter fatigue or failure. Channel #3 data appear normal and of high quality. For this reason only data from this last channel was analyzed and used for detailed comparison with theory. All MA-088 data have been binned into 30-s intervals, corresponding to the time necessary for the LOS to traverse at most one field width. During each such interval we separately treated data taken when the gas absorption cell was full and empty, and ignored data taken while the cell pressure was changing. In order to eliminate spikes of extraneous noise and telemetry dropouts from the data, we subjected each bin of 0.1-s data samples to a filtering process in which the mean and standard deviation of each set of samples was calculated, and then all samples more than three standard deviations away from the mean were discarded. The process was repeated until no more samples were discarded. The amount of data thereby eliminated was less than five per cent and was consistent with Poisson statistics. The resulting count rates for the various bins ranged between 2 and 60 counts s^{-1} at night and 12 to 1880 counts s^{-1} in the daytime. The standard deviations obtained from the statistics of the individual 0.1-s data samples were consistent with those expected from Poisson statistics.

We corrected the observed count rates for atmospheric absorption of 584 Å flux along the lines of sight by using the atmospheric models of

Jacchia (1971) and the 584 Å absorption cross-sections of Hall, Schweizer, and Hinteregger (1965) for N₂, O and O₂. Our calculations were based on the spacecraft position and LOS orientation at the mid-point of each bin. The solar activity parameters required as inputs to the Jacchia models were taken from Lincoln (1975). The effect of these corrections was to increase the observed flux levels by 10 to 30 per cent.

It is also necessary to allow for resonant absorption of 584 Å flux by the $1-2 \times 10^{14}$ atoms cm⁻² (Jacchia 1971) of atmospheric helium remaining above the spacecraft. This correction is model-dependent, for it depends on the spectral profile of the 584 Å line scattered from the ISM helium. Therefore, we chose to incorporate this correction into the models used for predicting the scattered line.

2. APPLICATIONS OF THE HGD DATA

2.1 The Nighttime 584 Å Emission.

To make certain that our conclusions about flux scattered from the local interstellar medium at night were not affected by daytime 584 Å radiation, we restricted the analysis in this case to data taken when the Sun was at least 30° below the horizon. Since the Earth's limb is depressed 15° below the horizontal when viewed from 220 km altitude, this constraint corresponded to a solar zenith angle of at least 135°. To minimize the affect on our analysis of errors in calculating absorption of 584 Å flux by the atmosphere above 220 km, we chose to analyze only those data for which the zenith angle of the LOS was less than 60°. Finally, we excluded

from analysis data taken when the spacecraft was in the South Atlantic Anomaly. After these three constraints were imposed, 53 minutes of data remained for study.

We investigated the possibility of other terrestrial phenomena affecting the data by correlating the binned, absorption-corrected data with LOS zenith angle, solar zenith angle, LOS-Sun angle, local strength of the geomagnetic field, magnetic latitude, and component of spacecraft velocity along the LOS. The only correlation we found at night was with magnetic latitude. There is a pronounced increase in count rates south of magnetic latitude -50° , and a noticeable peak within 10° of the magnetic equator. These increased count rates may be due to localized airglow such as that reported by Carruthers and Page (1972), or to some other cause. We decided to restrict the data under analysis further, by excluding data taken south of magnetic latitude -50° or within 10° of the magnetic equator. After this additional exclusion there remained 42 minutes of data.

We encountered one more problem in reducing the data. As discussed by Schmidtke (1976), the total solar 584 \AA flux varies from day to day by as much as thirty per cent. This short-term variability appears to be sufficiently unsystematic that we are reluctant to interpolate between Schmidtke's published data points, which are spaced at least 24 hours apart. We are not aware of any studies of solar 584 \AA variability on shorter time scales.

The 42 minutes of Apollo-Soyuz data we have selected for analysis

are composed of eight separate intervals, 1-10 minutes long, spaced 1-24 hours apart. To allow for possible solar 584 Å flux variations from interval to interval, we decided to allow the assumed value of that flux to vary, from interval to interval, while searching for model fits.

The by now conventionally accepted modified cold model (MCM) of ISM flow through the solar system was used to attempt to interpret these data via model-fitting. The cold model phase-space density function derives from the assumption that the distant ISM has a temperature of zero; that is, that all atoms move in the same direction with the same speed. Given a point near the Sun, not located on the axis of symmetry, it can be shown that only two orbits with the zero-temperature initial conditions cross that point.

If the selected point is directly upstream of the Sun only one orbit crosses it, but in the zero-temperature approximation every orbit crosses the downstream symmetry axis. This latter condition leads to an unphysical density spike at the downstream axis, and the cold model thereby falsely predicts a bright, localized EUV flux scattered from that region.

Feldman, Goldstein and Sherb (1972) and Blum, Pfleiderer and Wulf-Mathies (1975) have published formulae for altering the number density function close to the downstream axis to take first-order account of non-zero atomic thermal speeds. With the addition of such formulae, the cold model becomes the modified cold model.

In this model, the three-dimensional integral over gas velocity collapses to a two-term sum, and Dirac delta functions allow the integrations on frequency to be performed immediately. The evaluation of the flux I in

this model is thereby reduced to a one-dimensional numerical integration along the line of sight; which can be accomplished quickly on even a small computer.

We have used this modified cold model to attempt to explain the HGD observations. No reasonable fits to the data were found. This is probably due to the fact that the cold model is valid only when the thermal gas speeds are small compared to the bulk speed. The ASTP HGD instrument is highly sensitive, however, to the dynamical state of the gas. Thus the inability of the cold model to explain the data must be taken to indicate that the instrument is far too sophisticated for such a simple model and to make any progress a better model must be used.

We have developed this model and have applied it to the HGD observations. A brief description of this model (which we call the hot model) is given in paragraph 3 of this report and a more detailed analysis of it may be found in paper 6.3 in the appendix.

The hot model predictions were again compared to the HGD data in a manner similar to that used unsuccessfully with the cold model. Details of this analysis may be found in paper 6.1 in the appendix to this report.

In brief, we evaluated the hot model predictions for the physical parameters corresponding to the mid-points of the various HGD data bins. In all cases, the cell-full count rates and predictions were substantially less than the corresponding cell-empty values. Almost all cell-empty flux predictions increased with temperatures as did most cell-full predictions. During one interval of data collection, the cell-full predictions were

extremely low, between 0.001 and 0.06 rayleigh, while the actual count rates detected by the instrument were 2 or 3 per second. If these count rates were caused by helium 584 Å flux, they correspond to fluxes of 0.1-0.2 rayleigh. The adjustment to the linear factors F_v and n_{He} required to make the model predictions fit these data is about ten times larger than that required by any other combination of predictions and data, including the cell-empty case for the same interval. Therefore, we conclude that these cell-full counts were not caused by 584 Å flux. Instead, we believe the instrument observed several counts per second of background flux of unknown wavelength. We cannot determine the number of rayleighs of this radiation present, since the calibration of our detector varies with wavelength.

We then proceeded with the fitting of the data to the model predictions. First, we subtracted from each data point a constant 2.5 counts per second, to correct for the background count rate detected. Second, we converted the resulting count rates to rayleighs of flux by dividing by the instrument 584 Å sensitivity of 18 counts s^{-1} rayleigh $^{-1}$. Finally, for each discrete interval of data collection, we determined the appropriate factor by which the nominal product $n_{He} F_o$ must be multiplied to best fit (minimum chi-square) the envelope of predictions to the observed fluxes. We call this quantity the scale factor. The observed fluxes, with background removed, and the scaled model predictions, are displayed in Figures 1-2, which correspond to the eight distinct intervals of data collection which we have discussed. The envelopes of the model predictions are indicated by

shading. Solid lines, with representative error bars, depict the observed fluxes. The error bars do not reflect calibration errors of the instrument, since these presumably result only in an unknown, constant correction to the nominal instrument sensitivity of $18 \text{ counts s}^{-1} \text{ rayleigh}^{-1}$, which will automatically be factored out in determining the scale factors.

The specific scale factor used for each Figure is displayed below the ordinate, and measures the amount by which the product of the solar 584 \AA flux F_{\odot} and the interstellar neutral helium density n_{He} assumed in the model differed from that actually present. Thus a scale factor of 0.5 means that the product $n_{\text{He}} F_{\odot}$ actually present was half that assumed by the model. The scale factors vary from 0.63 to 0.84.

The only background allowed for in our data reduction was a Poisson-distributed random term with constant mean rate $2.5 \text{ counts s}^{-1}$. If variations in the background sources mentioned caused that mean rate to change during the intervals of data collection, then the Poisson variances which we have used in calculating chi-square are too small. Variations in mean background rate of as little as 3 counts s^{-1} would increase the variances by factors of 1.5 to 4 and thereby reduce the calculated chi-squares by about a factor of two. The background sources just discussed are more than sufficient to account for such variations, although their quantitative behavior is insufficiently known to make more precise calculations of their effects on chi-square.

In light of these background sources, we believe that our new model reasonably describes the HGD data.

The average scale factor for the eight distinct intervals of data collection is 0.76 ± 0.06 . Thus, if our model predictions are to agree, on the average, with the reduced observations, we must adjust the values of n_{He} and F_{O} so that their product is 0.76×10^7 photons $\text{cm}^{-5} \text{s}^{-1}$.

There has been much discussion of the correct average value of the solar 584 Å flux F_{O} . Hall and Hinteregger (1970) reported $F_{\text{O}} = (8.9 \pm 1.8) \times 10^8$ photons $\text{cm}^{-2} \text{s}^{-1}$ and Hinteregger (1976) has recently revised this value upward by 30-60 per cent. Rusch et al. (1976) have tabulated Atmospheric Explorer C observations for 1974 June 8, showing $F_{\text{O}} = (15.5 \pm 4.7) \times 10^8$ photons $\text{cm}^{-2} \text{s}^{-1}$. Maloy et al. (1975), observing on 1974 November 27, found $F_{\text{O}} = (26 \pm 3) \times 10^8$ photons $\text{cm}^{-2} \text{s}^{-1}$, and have later (Carlson 1976) revised the uncertainty to 30 per cent. Heroux and Higgins (1977) reported values of F_{O} between 13 and 15 $\times 10^8$ photons $\text{cm}^{-2} \text{s}^{-1}$, on five separate occasions from 1971 to 1976. To encompass these diverse results, we shall adopt $F_{\text{O}} = (20 \pm 10) \times 10^8$ photons $\text{cm}^{-2} \text{s}^{-1}$ as an appropriate average value for the remainder of this discussion.

Since the product $n_{\text{He}} F_{\text{O}}$ must equal 0.76×10^7 photons $\text{cm}^{-2} \text{s}^{-1}$, we conclude that $n_{\text{He}} = (3.8 \pm 2.1) \times 10^{-3} \text{cm}^{-3}$. The error given is the root sum square of the error assumed in F_{O} , the calibration error of the instrument, and the standard deviations calculated in averaging the scale factors. Consequently, three major conclusions follow from the analysis of the Apollo-Soyuz nighttime 584 Å helium observations. First, the total solar 584 Å flux may vary by as much as 20 per cent on a time scale as short as an hour or less. Second, the data and analysis generally support most recent conclusions about local ISM parameters derived from observations of resonantly scattered solar EUV flux. More specifically, our observations

are consistent with the interstellar gas moving toward $\alpha = 72^\circ$, $\delta = +15^\circ$, at a distant bulk speed of 20 km s^{-1} , with a temperature of 5000–20,000 K. Third, the neutral helium number density in the local ISM is $(3.8 \pm 2.1) \times 10^{-3} \text{ cm}^{-3}$.

It is clear that future interpreters of 584 \AA observations of the local ISM must be most cautious in drawing conclusions based on exact values of the solar 584 \AA flux without near-simultaneous full-disc measurements of that quantity.

The fact that our model fits were obtained with values of the ISM parameters generally similar to those recently used by other authors is more than a mere confirming observation, for as we have discussed above, most previous analysis of helium 584 \AA observations has been by means of a model strictly valid only for very low ISM temperatures. Our model does not possess this restriction, and so the broad agreement of our analysis with those which preceded it reduces the possibility that the previously obtained fits of a low-temperature model to a high-temperature gas may have in some way been specious or misleading.

The value of n_{He} which we report is consistent with more recent conclusions. Freeman et al. (1977) concluded $n_{\text{He}} \leq (0.004 \pm 0.0022) \text{ cm}^{-3}$ on the basis of observations made during the Apollo-Soyuz mission, with a different instrument. Fahr, Lay and Wulf-Mathies (1977) have supported this conclusion. Given the nominal 0.085 relative cosmic abundance of helium atoms to hydrogen atoms (Allen 1973a), our value for n_{He} implies a number density n_{H} of neutral hydrogen in the nearby ISM of $0.045 \pm 0.025 \text{ cm}^{-3}$.

2.2 The Daytime He I, 584 \AA Emission.

Some of the MA-088 channel #3 data were taken while the Sun was well above the horizon. These data have been examined to see whether the daytime count rates, which are much higher than the nighttime rates, can be explained by airglow lines of helium or of other atmospheric species. The results of this analysis are described in detail in a paper prepared for publication in the Journal of Geophysical Research and appended to this report as Paper 3.

We imposed several additional constraints on the data selected for analysis and discussion for this case. We required that the line of sight point within 97° of the local zenith, which corresponds to the lower edge of the field of view being tangent to the Earth's limb. We excluded data taken in or near the South Atlantic Anomaly. And to avoid contamination by sunlight reflected from the spacecraft, we included only data taken when the line of sight pointed more than 60° from the Sun. These conditions were met by a total of 1105 seconds of data, all taken on July 20 or 21, 1975, from an orbital altitude of about 225 km.

With gas absorption cell empty, the count rates detected ranged from 81 to 1880 counts s^{-1} . With the cell filled, the corresponding range of rates was 12 to 811 counts s^{-1} . We correlated the reduced cell-full and cell-empty data with several parameters upon which airglow intensities might depend, including solar zenith angle, line-of-sight elevation, and angle between line of sight and the Sun.

The only correlation we found was with solar zenith angle, which is also the angle in arc on the Earth's surface between the subsolar point

and the spacecraft position. In Figure 3 we show the cell-empty and cell-full count rates plotted against solar zenith angle, with typical error bars. The straight lines are linear regressions fits for the two cases. The r-square parameters for the two fits are 0.686 for the cell-empty data and 0.195 for the cell-full data. This dependence of the observed fluxes on spacecraft position is qualitatively consistent with the model of He I 584 Å scattering from an optically thick neutral helium geocorona, developed by Meier and Weller (1972).

As shown in Figure 3, the cell-full count rate tracked the cell-empty count rate remarkably well. Although the fluxes observed varied by an overall factor of twenty, the cell-full count rate remained at about 0.3 of the cell-empty count rate throughout.

This behaviour of the HGD data has permitted us to come to the following conclusions:

First, by subtracting cell-full from cell-empty count rates, we conclude that the daytime He I EUV geocoronal flux intensity spans the range 2-70 rayleighs. This value compares favorably with the 25 rayleighs of 584 Å flux reported by Christensen (1976) between 210 and 240 km at a solar zenith angle of 74°. We stress that because of the use of the gas absorption cell, our measurement is not contaminated by any radiation whose wavelength differs from the He I ground-state lines by more than a few mÅ. We also restate that our data set is limited by several constraints -- notably, the line of sight always points 60° or more from the Sun.

Second, inasmuch as the gas cell was designed to absorb all geocoronal

584 Å flux, the substantial 500-700 Å flux observed through the filled cell must have some other origin. Interplanetary 584 Å flux might be Doppler-shifted sufficiently to be transmitted by the gas cell, but the theoretical work cited indicates that this flux is much too weak to explain our cell-full data. We cannot calculate an absolute intensity for this radiation, since its wavelength or wavelengths, and hence the correct calibration factors for our detector, are not known.

Third, the strong correlation between the cell-full flux and such a local parameter as spacecraft position, suggests that this flux originated near the Earth. The intensity of this radiation varies with the observer's position in a manner similar to that of the 584 Å flux, at least for the range of observation positions and directions considered here.

Carruthers and Page (1972, 1976) and Christensen (1976) have reported possible detections of dayglow spectral lines between 600 and 700 Å with intensities comparable to He I 584 Å. Any of these lines might explain our cell-full fluxes. More detailed investigations with high-resolution spectrometers will be needed to define conclusively the spectral distribution of the radiation in this band.

3. A HOT MODEL OF THE INTERSTELLAR MEDIUM

In this work the distant ISM is described by a Maxwell-Boltzmann distribution of temperature T , moving with bulk speed V_B in a certain direction. This initial condition makes the analytical description of the phase-space number density function $n(v,s)$ a much more difficult problem. Furthermore, the use of such numerical techniques as Monte Carlo methods

to evaluate $n(v,s)$, requires large amounts of time on even the fastest of present-day computers. It is therefore not surprising that most workers in the study of the local ISM continued to use the modified cold model, even when early results indicated that thermal speeds might in fact not be small.

In 1975 Wallis pointed out that an analytic solution for $n(v,s)$ under the initial conditions just given had been obtained by Danby and Gamm in 1957, in the context of a different astrophysical problem. The Danby and Gamm expression for $n(v,s)$ contains an exponential of a complicated trigonometric function which is difficult to manipulate analytically. Furthermore, although Dirac delta functions in $a(v_*, v, v_1)$ allow two of the integrations to be performed immediately, the calculation of an observed flux using the Danby and Gamm $n(v,s)$ nevertheless requires a four-dimensional integration, three dimensions more than with the modified cold model.

We have developed a program to evaluate the scattered intensity by numerical integration, using the Danby and Gamm number density function, modified by the inclusion of the factor $\exp(-\beta_0 r_E^2 \theta / V_B p)$ which was used by preceding authors (e.g. Blum, Pfeleiderer and Wulf-Mathies 1975) to allow for the loss of gas atoms by ionization due to solar EUV. In this factor, β_0 is the rate at which gas atoms are ionized at one astronomical unit r_E from the Sun, θ is the angle through which a gas atom has orbited about the Sun, and p is the impact parameter of the orbit in question. We refer to this model as the hot model.

Our hot model uses Simpson's rule to perform all four integrations.

In testing the program, we varied the number and spacing of points at which the integrand was evaluated, until we observed an apparent asymptotic limit to the calculated value of the scattered flux I . For all further work, we used a number and spacing of points which produced a value of I within ten per cent of the observed limit. We checked the program validity by using several limiting cases singly and in combination, such as setting solar mass and radiation pressure equal to zero, letting $\Delta\lambda$ approach infinity, and allowing T to trend toward zero. Calculations using the program also display symmetries reflecting the geometrical symmetries of the physical situation involved.

The program provides the total observed flux and the observed line profile. It has provision for also calculating the flux and line profile observed when a helium gas absorption cell is interposed between the observer and the line of sight. We have so far used the program to investigate the behavior of neutral helium as observed via the resonant scattering of solar EUV at 584 \AA as it pertains to our HGD data. Each evaluation of the integral (1) requires three to fifteen minutes of central processor time on a CDC 6400 computer.

Fourteen physical parameters determine the predictions of the models. These are three parameters describing the bulk velocity of the distant gas, the distant gas temperature T and neutral helium number density n_{∞} , the rate β_0 at which the gas is ionized at one A.U. from the Sun, the FWHM $\Delta\lambda$ of the solar resonance line, the solar line flux F_0 at one A.U. from the Sun, the ratio μ of the pressure of light to the force of solar gravity

on a gas atom, three parameters characterizing the position of the observer and two describing the line of sight (LOS) of the observation,

The results of this work demonstrate that when the modified cold model and the newly developed hot model predictions for helium atoms are evaluated for physical parameters in the range presently believed correct, the hot model predicts broader intensity maxima and smaller total variations in flux level than does the modified cold model. The shapes of the intensity maxima are sufficiently complicated that the difference in shape is difficult to quantify, but our calculations indicate that the patterns of 584 \AA glow predicted by the two models are markedly different within 60 to 90° away from the projection of the downwind symmetry axis on the celestial sphere. We conclude that the modified cold model should not be used to analyze observations of this region.

At greater distances from the downwind axis, the shapes and spacings of the isophotes predicted by the two models are more similar, although the hot model predicts several times as much flux as the modified cold model. The modified cold model may possibly be of use for interpreting observations of this part of the sky, provided the analysis used depends only on the relative intensities of flux observed from different points. Future observers of 584 \AA helium glow should address the question of model validity more specifically.

The hot model predicts substantial variations of observed flux with temperature, on lines of sight for which the modified cold model predicts no variation at all. Furthermore, even when the modified cold model does predict a variation of flux with temperature, the hot model predicts

variations of a different kind. The use of the modified cold model to determine the precise temperature of the local ISM therefore appears invalid.

The conclusions drawn by previous observers of 584 \AA flux who have used the modified cold model to interpret their data must be reassessed. The hot model does not fit the data of Weller and Meier (1974) as well as the modified cold model did. We therefore suggest that further study of both model and data is in order, to determine the cause of the discrepancy and the actual values of the ISM parameters that the data imply. When the hot model is used to analyze the data of Freeman et al. (1976) the derived lower limit to gas bulk speed is slightly nearer to the values of V_b obtained by other means than was the case with the modified cold model.

The theoretical question of the behavior of the local ISM is far from closed. Both the modified cold model and the hot model derive from two assumptions. First, the flow of the ISM through the solar system is assumed to be collisionless, so that each atom proceeds along a hyperbolic orbit determined by celestial mechanics. Second, the nearby ISM is assumed sufficiently tenuous that only singly-scattered photons will reach the observer. Wallis (1973, 1974, 1975) has questioned both of these assumptions. Further analytic and numerical study of their validity may be necessary before experimenters can have complete confidence in the interpretation of 584 \AA data.

REFERENCES

- Allen, C. W., 1964. Astrophysical Quantities, Athlone Press, London.
- Blum, P. W., Pfleiderer, J., and Wulf-Mathies, C., 1975, Planet. Space Sci., 23, 93.
- Carlson, R. W., 1976. Private communication.
- Carruthers, G. R., and Page, T., 1972. Science, 177, 788.
- _____, 1976. J. Geophys. Res., 81, 1683.
- Christensen, A. B., 1976. Geophys. Res. Letters, 3, 221.
- Danby, J. M. A., and Camm, G. L., 1957, Mon. Not. R. Ast. Soc., 117, 50.
- Fahr, H. J., Lay, G., and Wulf-Mathies, C., 1977. Paper presented at COSPAR meeting XX, Tel Aviv, Israel.
- Feldman, W. F., Goldstein, D., and Sherb, F., 1972, J. Geophys. Res., 77, 5389.
- Freeman, J., Paresce, F., Bowyer, S., and Lampton, M., 1976. Ap. J., 208, 747.
- Freeman, J., Paresce, F., Bowyer, S., Lampton, M., Stern, R., and Margon, B., 1977. Ap. J. (Letters), 215, L83.
- Hall, L. A., and Hinteregger, H. E., 1970. J. Geophys. Res., 75, 6959.
- Hall, L. A., Schwiezer, W., and Hinteregger, H. E., 1965. J. Geophys. Res., 70, 105.
- Heroux, L., and Higgins, J. E., 1977. J. Geophys. Res., 82, 3307.
- Hinteregger, H. E., 1976. J. Atm. Terr. Phys., 38, 791.
- Jacchia, L. G., 1971. Smithsonian Ap. Obs. Spec. Rept., No. 332.
- Lincoln, J. V., 1975. J. Geophys. Res., 80, 4773.
- Maloy, J. O., Carlson, R. W., Hartman, V. C., and Judge, D. W., 1975. Paper presented at the 1975 Fall Annual Meeting of the American Geophysical Union, 1975 December.
- Meier, R. R., and Weller, C. S., 1972. J. Geophys. Res., 77, 1190.

- Rusch, D. W., Torr, D. G., Hays, P. B., and Torr, M. R., 1976. Geophys. Res. Letters, 9, 537.
- Schmidtke, G., 1976. Geophys. Res. Letters, 10, 573.
- Wallis, M. K., 1973. Astrophys. & Space Sci., 20, 3.
- _____, 1974. Mon. Not. R. Astr. Soc., 167, 103.
- _____, 1975. Planet. Space Sci., 23, 419.
- Weller, C. S., and Meier, R. R., 1974. Astrophys. J., 193, 471.

FIGURE CAPTIONS

Figures 1-8: Reduced observed fluxes and model predictions for the eight discrete intervals of data collection. Open circles = cell-empty fluxes. Solid circles = cell-full fluxes. Representative error bars are shown. Shaded area = envelope of model predictions as temperature varies from 5000 to 20,000 K. The model predictions have been adjusted so that the product $n_{\text{He}} F_{\text{O}} = A \times 10^{-7}$ photons $\text{cm}^{-5} \text{s}^{-1}$, where the value of A is displayed at the bottom of each Figure.

Figure 9: Cell-full (lower) and cell-empty (upper) count rates versus solar zenith angle. Calculated linear regressions fits shown by diagonal lines.

RAYLEIGHS

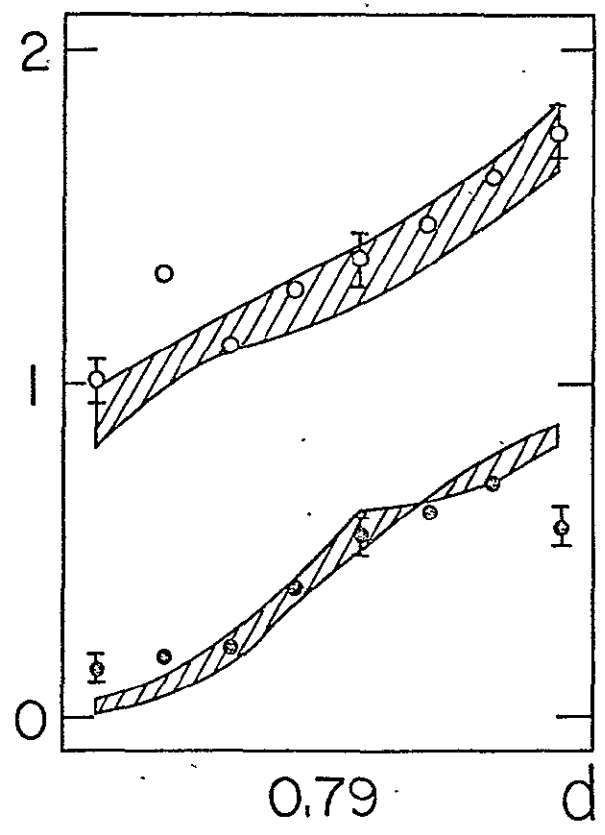
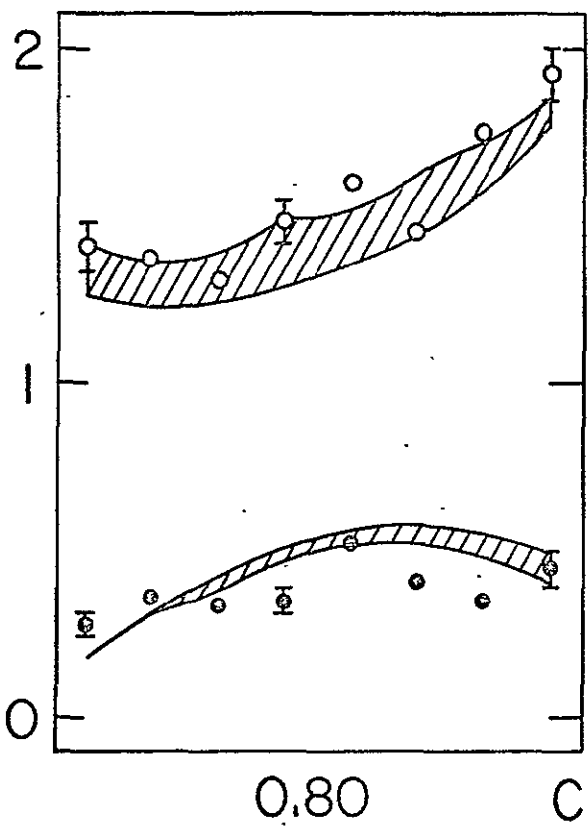
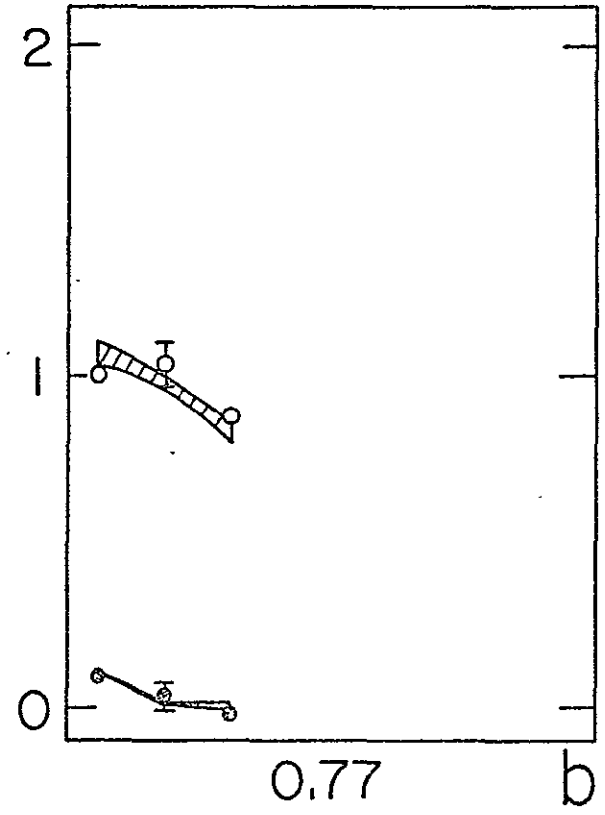
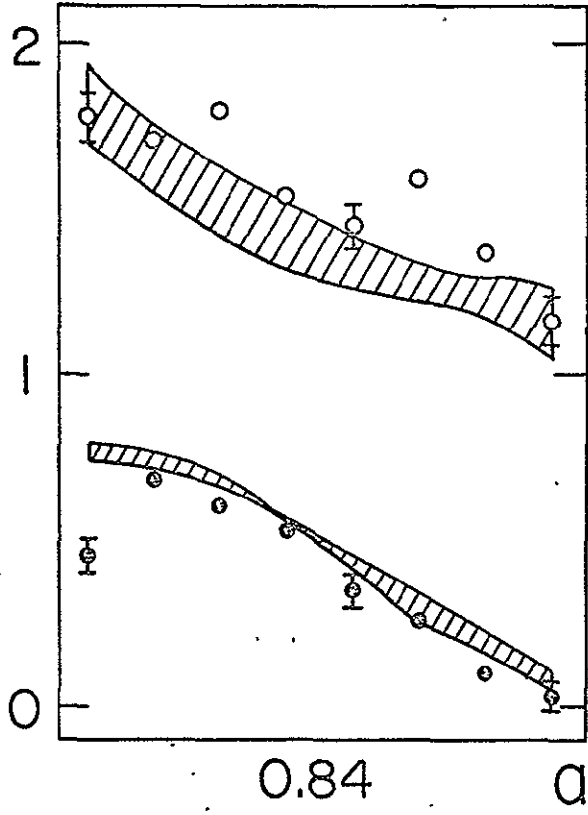


Figure 1.

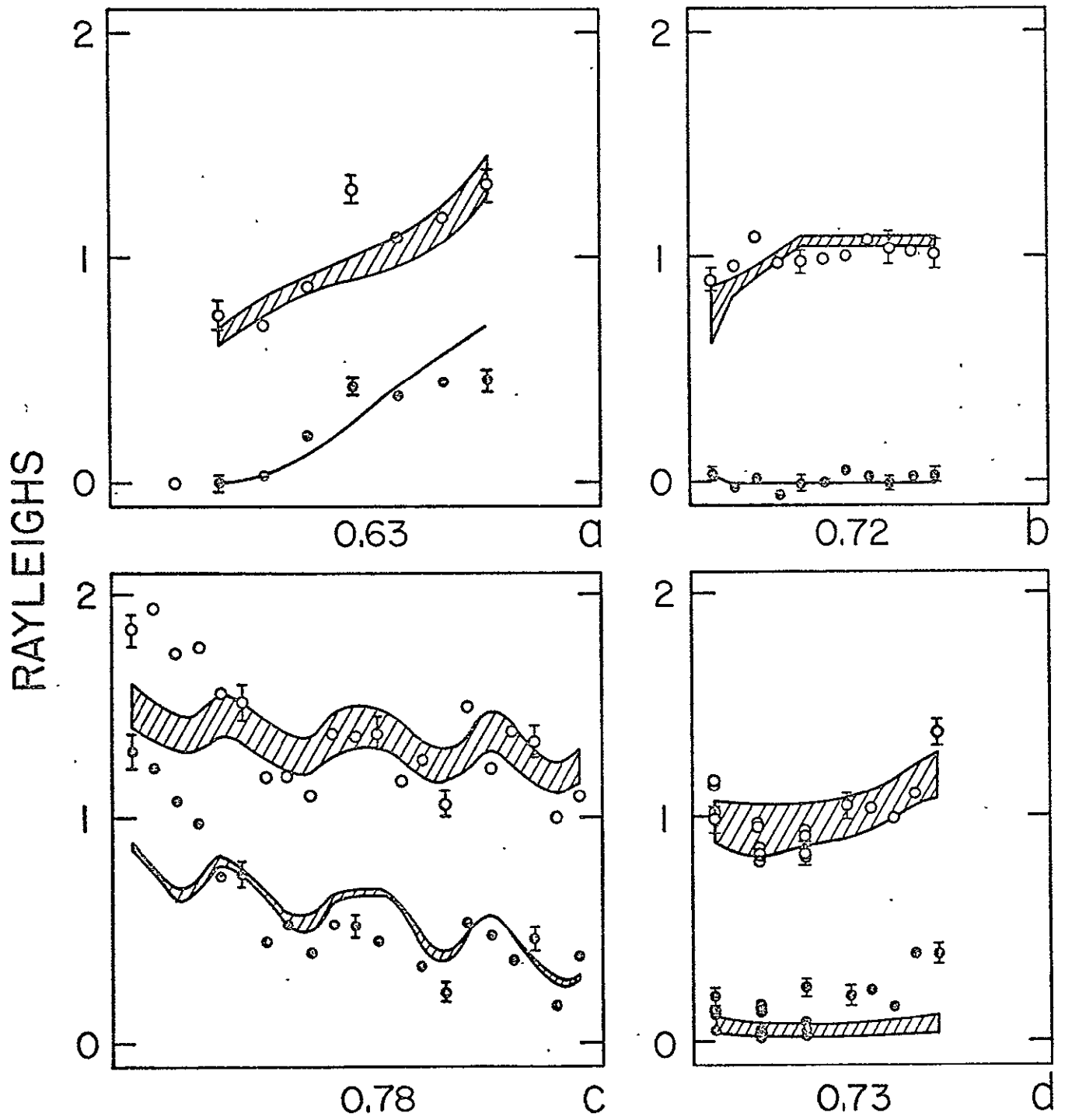


Figure 2.

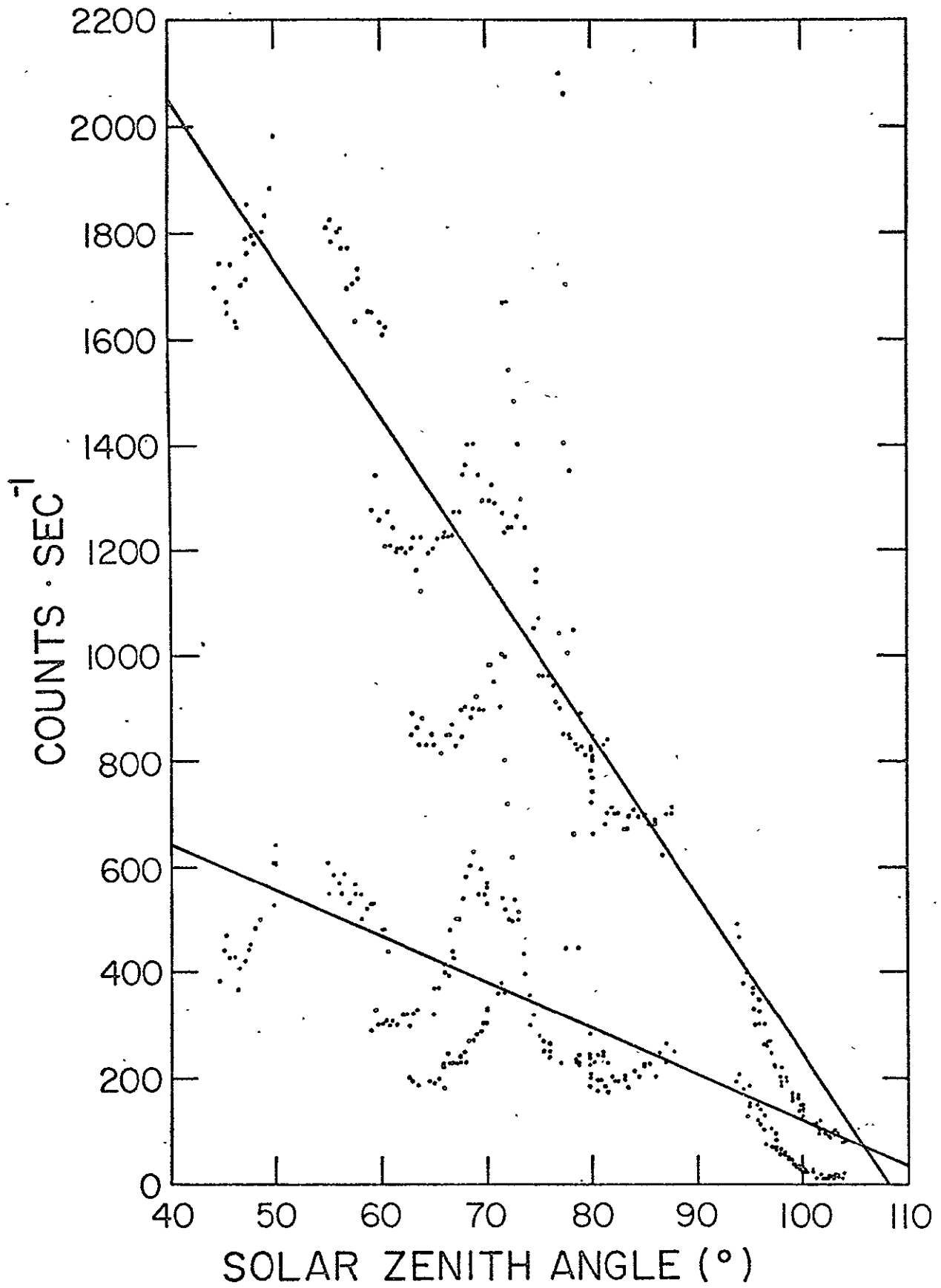


Figure 3.

OBSERVATIONS OF INTERSTELLAR HELIUM WITH A GAS ABSORPTION CELL:
IMPLICATIONS FOR THE STRUCTURE OF THE LOCAL INTERSTELLAR MEDIUM

Jay Freeman, Francesco Paresce
Stuart Bowyer, and Michael Lampton

Space Sciences Laboratory
University of California
Berkeley, California 94720

ABSTRACT

A photometer sensitive at the 584 Å line of HeI, incorporating a helium gas resonant absorption cell, was flown on the Apollo-Soyuz Test Project in July 1975. The instrument observed much of the nighttime sky, and returned 42 minutes of useable data. The data were analyzed by fitting to a model of resonant scattering of solar 584 Å flux from nearby interstellar helium, which is valid even when the interstellar gas is hot. Good model fits were obtained for an interstellar gas bulk velocity vector pointing toward $\alpha = 72^\circ$, $\delta = +15^\circ$, with speed 20 km s^{-1} ; with interstellar medium temperatures from 5000 to 20,000 K and with neutral interstellar helium density $0.0038 \pm 0.0021 \text{ cm}^{-3}$. The results are consistent with the Sun lying in the warm, partially ionized periphery of a cold interstellar cloud surrounded by old supernova remnants, as described by McKee and Ostriker (1977).

1. INTRODUCTION

Observations of interstellar gas passing through the solar system provide information about the temperature, number density, composition and bulk velocity of the local interstellar medium (ISM). A number of authors (Blum and Fahr 1970; Holzer and Axford 1971; Axford 1972; Johnson 1972; Paresce and Bowyer 1973; Wallis 1973, 1974, 1975; Meier 1977; Freeman and Paresce 1978) have described how neutral atoms passing near the Sun are gravitationally focused into a density distribution whose shape depends in a complicated manner both on physical parameters of the ISM and on the local effects of photoionization by the Sun, collisional ionization and heating by the solar wind, collisions with other atoms, and the pressure of sunlight. Study of the details of this distribution allows untangling of the various parameters by model fitting. Studies of the distribution of the local ISM have been made by observation of solar ultraviolet and extreme ultraviolet (EUV) light scattered by hydrogen (Bertaux and Blamont 1971; Thomas and Krassa 1971; Thomas 1972; Bertaux et al. 1976), and helium (Paresce, Bowyer and Kumar 1973a,b, 1974; Weller and Meier 1974; Freeman

et al. 1976a, 1977; Ajello 1977). These experiments have established the direction toward which the local ISM moves as within about fifteen degrees of $\alpha = 72^\circ$, $\delta = +15^\circ$, and have determined the bulk speed of the distant gas to be within a few km s^{-1} of 20, but there remains a somewhat greater controversy about the temperature and number density of the gas.

There has been a substantial theoretical difficulty with the models used to interpret the data from these experiments. Most observers of helium have performed their model-fitting using a model which is strictly valid only if the thermal speeds of individual atoms are very small compared to the bulk speed of the distant gas. At a temperature of 10^4 K, roughly the mid-point of the range discussed in the references cited, the actual helium thermal speed is 4.6 km s^{-1} , whereas the bulk speed V_B seems to be about 20 km s^{-1} , as discussed above. There is therefore room for doubt about the applicability of the low-temperature models and the accuracy of conclusions derived by using them. Models valid at higher temperatures are analytically complicated and require large amounts of computer time to evaluate, and have only recently become available (Meier 1977; Freeman and

Paresce 1978). In the present work, we use the model of Freeman and Paresce to interpret data obtained with a 584 Å photometer, equipped with a helium gas resonant absorption cell, during the 1975 Apollo-Soyuz Test Project.

II. INSTRUMENTATION

Complete details of the construction and calibration of the Apollo-Soyuz helium 584 Å photometer have been published elsewhere (Bowyer et al. 1977). In brief, the instrument consisted of a channel electron multiplier (CEM) whose optical axis traversed a gas cell 10 cm long. The cell was sealed by metal foil EUV filters, one tin and one aluminum, each approximately 1200 Å thick. The cell was alternately filled with helium at a pressure of 1.4 torr for a period of approximately 2.5 s, and then vented to space for an equal interval. The helium column density within the filled cell was 4.9×10^{17} atoms cm^{-2} . The helium column absorbed more than 99 per cent over a band about 40 mÅ full width, centered on the 584 Å line. This absorption feature was sufficiently broad to absorb solar 584 Å flux scattered by neutral helium in the Earth's upper atmosphere, even at several times the nominal (Jacchia 1971) exospheric temperature of 10^3 K, and even

when that scattered flux was Doppler-shifted by the entire 8 km s^{-1} orbital speed of the spacecraft.

When the cell was vented, the partial pressure of helium within it was calculated to fall to less than 10^{-6} torr in a few tenths of a second, which corresponds to a helium column density not exceeding 3×10^{11} atoms cm^{-2} .

At this column density the absorption feature would have had a full width at half maximum of $2 \text{ m}\text{\AA}$ and a maximum absorption, at line center, of 12 per cent of the incident flux. Such an absorption feature is narrow compared with the calculated profiles of the solar 584 \AA line scattered from the local ISM. Hence absorption caused by the vented gas cell was negligible.

An end-to-end photometric calibration of the instrument was performed before flight, using emission lines of hydrogen, helium, neon, and argon at wavelengths of 200 to 2000 \AA . NBS-calibrated Al_2O_3 photodiodes and gas proportional counters were used as reference standards. With gas cell vented, the instrument sensitivity to diffuse 584 \AA flux was $18 \pm 3.6 \text{ counts s}^{-1} \text{ rayleigh}^{-1}$. The product of CEM quantum efficiency and metal foil filter transmissions was 4×10^{-3} , and the field of view was approximately 14 degrees

in diameter. In the laboratory, the instrument exhibited a dark count rate of less than 0.1 count s^{-1} . A comparable count rate was obtained in flight with the instrument door closed.

III. DATA

The Apollo spacecraft carrying our instrument was launched in July, 1975, into a near-circular orbit at 220 km altitude. The orbital plane was inclined at 55° to the celestial equator, and approximately contained the Earth-Sun line. Data were taken at various times during the mission while the spacecraft was maneuvered so that the instrument field of view surveyed most of the celestial sphere. The instrument was also turned on at other times to acquire additional data from random lines of sight. The instrument was not operated during or immediately after purges of gas or liquid from the spacecraft, or when the reaction control system rocket motors nearest the instrument were activated. Approximately ten hours of data were obtained. NASA provided detailed spacecraft aspect and trajectory information for this time period.

Inspection of the data revealed that the observed count rates were 100-1000 times as large when the Sun was above the horizon as when it was

below the horizon. We ascribe these high daytime count rates to scattering of solar EUV radiation from residual atmosphere at and above the spacecraft orbit, and have discussed the matter in detail elsewhere (Freeman et al. 1978). To make certain that our conclusions about flux scattered from the local ISM were not affected by this daytime radiation, we restricted the present analysis to data taken when the Sun was at least 30° below the horizon. Since the Earth's limb is depressed 15° below the horizontal when viewed from 220 km altitude, this constraint corresponded to a solar zenith angle of at least 135° . To minimize the affect on our analysis of errors in calculating absorption of 584 \AA flux by the atmosphere above 220 km, we chose to analyze only those data for which the zenith angle of the line of sight (LOS) was less than 60° . Finally, we excluded from analysis data taken when the spacecraft was in the South Atlantic Anomaly. After these three constraints were imposed, 53 minutes of data remained for study.

While these data were being collected, the LOS scanned the sky at a rate of at most 0.5° s^{-1} . We therefore deemed it appropriate to bin the data into 30-s intervals, corresponding to the time necessary for the LOS to

9

traverse at most one field width. During each such interval we separately treated data taken when the gas absorption cell was full and empty, and ignored data taken while the cell pressure was changing. In order to eliminate spikes of extraneous noise and telemetry dropouts from the data, we subjected each bin of 0.1-s data samples to a filtering process in which the mean and standard deviation of each set of samples was calculated, and then all samples more than three standard deviations away from the mean were discarded. The process was repeated until no more samples were discarded. The amount of data thereby eliminated was less than five per cent and was consistent with Poisson statistics. The resulting count rates for the various bins ranged between 2 and 60 counts s^{-1} . The standard deviations obtained from the statistics of the individual 0.1-s data samples were consistent with those expected from Poisson statistics, and were generally in the range 0.5 - 1.5 counts s^{-1} .

We corrected the observed count rates for atmospheric absorption of 584 Å flux along the lines of sight by using the atmospheric models of Jacchia (1971). The solar activity parameters required as inputs to the

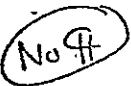
models were taken from Lincoln (1975). We used the 584 Å absorption cross-sections of Hall, Schweizer, and Hinteregger (1965) for N₂, O and O₂. Our calculations were based on the spacecraft position and LOS orientation at the mid-point of each bin. The effect of these corrections was to increase the observed flux levels by 10 to 30 per cent. We have not included in our stated errors the effect of any errors in the Jacchia models or the 584 Å absorption cross-sections of N₂, O and O₂.

It was also necessary to allow for resonant absorption of 584 Å flux by the $1-2 \times 10^{14}$ atoms cm⁻² (Jacchia 1971) of atmospheric helium remaining above the spacecraft. This correction is model-dependent, for it depends on the spectral profile of the 584 Å line scattered from the ISM helium. Therefore, we chose to incorporate this correction into the models used for predicting the scattered lines, which we shall describe in the next section.

We investigated the possibility of other terrestrial phenomena affecting the data by correlating the binned, absorption-corrected data with LOS zenith angle, solar zenith angle, LOS-Sun angle, local strength of the geomagnetic field, magnetic latitude, and component of spacecraft velocity along the LOS.

The only correlation we found was with magnetic latitude. In Figure 1 we show cell-empty count rates plotted against magnetic latitude. There is a pronounced increase in count rates south of magnetic latitude -50° , and a noticeable peak within 10° of the magnetic equator. These increased count rates may be due to localized airglow, particle precipitation, or some other cause. We decided to restrict the data under analysis further, by excluding data taken south of magnetic latitude -50° or within 10° of the magnetic equator. After this additional exclusion there remained 42 minutes of data. In Figure 2 we depict by hatching the portions of the sky viewed while these data were gathered.

We encountered one additional uncertainty in reducing the data. As discussed by Schmidtke (1976), the total solar 584 \AA flux varies from day to day by as much as thirty per cent. This short-term variability appears to be sufficiently unsystematic that we are reluctant to interpolate between Schmidtke's published data points, which are spaced at least 24 hours apart. We are not aware of any studies of solar 584 \AA variability on shorter time scales.

 ← The 42 minutes of Apollo-Soyuz data we have selected for analysis are

composed of eight separate intervals, 1-10 minutes long, spaced 1 to 24 hours apart. To allow for possible solar 584 Å flux variations from interval to interval, we decided to allow the assumed value of the flux to vary, from interval to interval, while searching for model fits.

IV. MODELING OF PHOTOMETRY OF THE LOCAL ISM

A general formalism describing radiation resonantly scattered from hydrogen and helium in the local ISM, in the approximation that thermal speeds of individual atoms are small compared to the bulk speed of the gas as a whole, is well established (e.g. Freeman et al. 1976a and references therein). We have recently described (Freeman and Paresce 1978) a revised model which does not require the approximation of small thermal speeds. The model evaluates the following integral for the observed flux I:

$$(1) \quad I = \int E(\nu_i) F(\nu_*, s) a(\nu_*, \vec{v}, \nu_i) p(\theta(s)) n(\vec{r}, s) d\Omega_* \frac{d\nu_i d^3v}{\nu_i^2}$$

In this integral, I is the number of photons detected per second by the

instrument, ν_i is the radiation frequency in an inertial frame attached to

the Sun, s is path length along the LOS, and \vec{v} is gas velocity. The quantity

$E(\nu_i)$ is instrument sensitivity as a function of wavelength, $F(\nu_*, s)$ is the

solar flux at the point described by s, $a(\nu_*, \vec{v}, \nu_i)$ is the total cross-

section for an atom moving with velocity \vec{v} to scatter light of frequency ν_* at the Sun in such a manner that the observer perceives its frequency as ν_i , $\theta(s)$ is the angle at s between the Sun and the observer, $p(\theta(s))$ is a phase function, and $n(\vec{v}, s)$ is the gas phase-space number density at s .

Our revised model differs from those which preceded it (except for the 1977 model of Meier) in that we use for $n(\vec{v}, s)$ an analytic expression due to Danby and Camm (1957), which is valid even for high temperatures of the distant ISM. Although Dirac delta functions in $a(\nu_*, \vec{v}, \nu_i)$ allow two of the integrations in equation (1) to be performed immediately, numerical solution of the remaining four-dimensional integral requires 3 to 15 minutes of central processor time on a CDC 6400 computer. Our program simultaneously evaluates equation (1) for two different functions $E(\nu_i)$, corresponding to gas absorption cell full and empty.

The predictions of the model depend on fifteen physical parameters, in addition to the function $E(\nu_i)$. The parameters describe the bulk speed V_B , temperature T , helium spatial number-density n_{He} and direction of motion of the distant gas, the position and LOS of the observer, the component of the

observer's velocity along the LOS, the total flux F_{\odot} of the solar 584 \AA line as measured at 1 AU from the Sun, the FWHM $\Delta\lambda$ of that line, the rate β_{\odot} at which neutral helium at 1 A.U. from the Sun is ionized by solar radiation at wavelengths less than 504 \AA , and the ratio μ between the pressure of sunlight and the force of solar gravity on a neutral helium atom.

For the modeling used in the present work, we assumed that the local ISM flows toward the direction $\alpha = 72^{\circ}$, $\delta = +15^{\circ}$, given by Weller and Meier (1974). Previous observations of the local ISM with gas absorption cells have placed limits on the gas bulk speed V_B . Bertaux et al. (1976), observing hydrogen, found V_B between 12.5 and 21 km s^{-1} , and most likely between 18 and 21 km s^{-1} . Freeman et al. (1976a), observing helium, found a lower limit of $10\text{--}15 \text{ km s}^{-1}$. Adams and Frisch (1977) have used Copernicus high-resolution spectrometer scans of Lyman-alpha background to measure the speed by Doppler shift, and found about 22 km s^{-1} . We therefore chose $V_B = 20 \text{ km s}^{-1}$ for our modeling.

Weller and Meier (1974) and Meier (1977) used $\Delta\lambda = 0.12 \text{ \AA}$ and $\beta_{\odot} = 6.8 \times 10^{-8} \text{ s}^{-1}$. Delaboudinière and Crifo (1975) summarize recent work indicating that $\Delta\lambda$ is between 0.11 and 0.15 \AA . Banks and Kockarts (1973) indicate that

$\beta_0 = (8.0 \pm 4.0) \times 10^{-8} \text{ s}^{-1}$, We selected $\Delta\lambda = 0.12 \text{ \AA}$ and $\beta_0 = 6.8 \times 10^{-8} \text{ s}^{-1}$ for the present work. We chose $\mu = 0$, as indicated by Fahr (1974), and we used values for the observer's position, velocity and LOS appropriate to the mid-points of the various data bins.

There is much uncertainty in the correct value of n_{He} , and as we have indicated, F_0 is known to vary substantially on a short time-scale. However, both of these quantities appear in the evaluation of (1) only as overall linear factors. Therefore, it is not necessary to justify the values used in the initial modeling, because the model predictions need only be scaled appropriately at a later stage in the analysis. We selected the numerically convenient values $n_{\text{He}} = 0.01 \text{ cm}^{-3}$ and $F_0 = 10^9 \text{ cm}^{-2} \text{ s}^{-1}$ for inputs to our computer program.

The work of Paresce, Bowyer, and Kumar (1974), Weller and Meier (1974), and Bertaux et al. (1976) suggests that T is within a factor of two or so of 10^4 K . Therefore, we evaluated our model for values of 5000, 10,000 and 20,000 K.

Finally, we corrected the 584 \AA line profiles predicted by the model

for resonant absorption by atmospheric helium above the spacecraft, using the atmospheric models of Jacchia (1971). The effect of this helium was to impose on the scattered lines an absorption feature typically $12 \text{ m}\text{\AA}$ FWHM, which absorbed more than 99 per cent of incident flux over a typical bandwidth of $10 \text{ m}\text{\AA}$. The feature was Doppler-shifted by the relative motion of the spacecraft to the atmosphere, but it was always contained within the absorption band produced by the filled helium gas absorption cell, and therefore could not alter the model predictions for cell-full flux,

The model predictions for the data discussed here were relatively insensitive to temperature, typically varying by less than 10 per cent as T was raised from 5000 to 20,000 K. This property is a straightforward consequence of the geometry of our observations. The lines of sight passed through only regions well upwind of the Sun, where the effects of temperature are known to be small (Freeman and Paresce 1978).

V. COMPARISON OF DATA AND MODEL PREDICTIONS

We evaluated the model predictions for the physical parameters corresponding to the mid-points of the various data bins. In all cases,

the cell-full count rates and predictions were substantially less than the corresponding cell-empty values. Almost all cell-empty flux predictions increased with temperature, as did most cell-full predictions.

We studied the non-584 Å background count rate by inspecting ^{those} observations for which our 584 Å models predicted a count rate of less than a few tenths of a count per second. During about 20 s of such observations, the background rate detected was 2.5 counts s⁻¹.

We then proceeded with the fitting of the data to the model predictions. First, we subtracted 2.5 counts per second from each data point to correct for the background rate. Second, we converted the resulting count rates to rayleighs of flux by dividing by the instrument 584 Å sensitivity of 18 counts s⁻¹ rayleigh⁻¹. Finally, for each discrete interval of data collection, we determined the appropriate factor by which the nominal product $n_{He} F_O$ must be multiplied to best fit (minimum chi-square) the envelope of predictions to the observed fluxes. We call this quantity the scale factor. The observed fluxes, with background removed, and the scaled model predictions, are displayed in Figures 3 and 4, which display the eight distinct intervals of

data collection which we have discussed. The envelopes of the model predictions are indicated by shading. Circles, with representative error bars, depict the observed fluxes. The error bars do not reflect calibration errors of the instrument, since these presumably result only in an unknown, constant correction to the nominal instrument sensitivity of $18 \text{ counts s}^{-1} \text{ rayleigh}^{-1}$, which will automatically be factored out in determining the scale factors. We shall include the effect of such calibration errors where appropriate in further analysis.

The specific scale factor used for each interval is displayed below the ordinate, and measures the amount by which the product of the solar 584 \AA flux F_{\odot} and the interstellar neutral helium density n_{He} assumed in the model differed from that actually present. Thus a scale factor of 0.5 means that the product $n_{\text{He}} F_{\odot}$ actually present was half that assumed by the model. The scale factors vary from 0.63 to 0.84. The scale factor used for each Figure is the average of the three separate scale factors obtained for best fits of the data to the model predictions for the three temperatures used. Each separate scale factor was derived by minimizing the chi-square statistic for the fit in question. We have scaled the predictions in the

Figures using the average scale factor, rather than using for each prediction the specific scale factor which minimizes its own chi-square, in order to display the variations in predictions with temperature more clearly,

The data displayed in Figures 3b and 4b are well-fit by the models, In Figure 3b, the minimum chi-squares for 5000, 10,000 and 20,000 K are respectively 2.69, 2.85 and 3.10, which imply confidence levels (with five degrees of freedom) of 0.75, 0.72, and 0.68 for the three temperatures respectively. In Figure 4b, there are 20 degrees of freedom and the minimum chi-squares are 30.59, 23.12, and 10.20 respectively. The confidence levels in this case are 0.06, 0.28, and 0.96 for 5000, 10,000 and 20,000 K respectively.

In all other figures, the chi-square fits are worse. Chi-square per degree of freedom ranges from 2 to 7, indicating very low confidence levels for the models. Spatial variations in the non-584 Å flux may have been responsible for much of this discrepancy. For example, a 3 counts s⁻¹ variation in this flux would decrease chi-square by a factor of two.

Possible sources of background counts include nighttime EUV airglow lines (Carruthers and Page 1972), geocoronal helium 584 Å radiation (Freeman

et al. 1976), and the unknown source which caused our high count rates near magnetic latitudes 0° and -50° . The spatial variations observed in these sources are more than sufficient to change the instrument background rate by several counts s^{-1} . Unfortunately, the quantitative details of these spatial variations are insufficiently known to permit more precise calculations of their effects on chi-square.

In light of these background sources, we believe that our models reasonably describe the data presented here. With the reductions in chi-square just discussed, the data do not rule out any of the three temperatures we used as model parameters.

The average scale factor for the eight distinct intervals of data collection is 0.76 ± 0.06 . Thus, if our model predictions are to agree, on the average, with the reduced observations, we must adjust the values of n_{He} and F_0 so that their product is 0.76×10^7 photons $\text{cm}^{-5} \text{s}^{-1}$,

There has been much discussion of the correct average value of the solar 584 \AA flux F_0 . Hall and Hinteregger (1970) reported $F_0 = (8.9 \pm 1.8) \times 10^8$ photons $\text{cm}^{-2} \text{s}^{-1}$ and Hinteregger (1976) has recently revised this value

upward by 30-60 per cent, Rusch et al, (1976) have tabulated Atmospheric Explorer C observations for 1974 June 8, showing $F_o = (15.5 \pm 4.7) \times 10^8$ photons $\text{cm}^{-2} \text{s}^{-1}$. Maloy et al. (1975), observing on 1974 November 27, found $F_o = (26 \pm 3) \times 10^8$ photons $\text{cm}^{-2} \text{s}^{-1}$, and have later (Carlson 1976) revised the uncertainty to 30 per cent. Heroux and Higgins (1977) reported values of F_o between 13 and 15 $\times 10^8$ photons $\text{cm}^{-2} \text{s}^{-1}$, on five separate occasions from 1971 to 1976. To encompass these diverse results, we shall adopt $F_o = (20 \pm 10) \times 10^8$ photons $\text{cm}^{-2} \text{s}^{-1}$ as an appropriate average value for the remainder of this discussion.

Since the product $n_{\text{He}} F_o$ must equal 0.76×10^7 photons $\text{cm}^{-5} \text{s}^{-1}$, we conclude that $n_{\text{He}} = (3.8 \pm 2.1) \times 10^{-3} \text{ cm}^{-3}$. The error given is the root sum square of the error assumed in F_o , the calibration error of the instrument, and the standard deviation calculated in averaging the scale factors.

VI. DISCUSSION AND CONCLUSIONS

Two major conclusions follow from the analysis of Apollo-Soyuz 584 Å helium observations presented here. First, the data and analysis generally

support most recent conclusions about local ISM parameters derived from observations of resonantly scattered solar EUV flux. Second, the neutral helium number density in the local ISM is $(3.8 \pm 2.1) \times 10^{-3} \text{ cm}^{-3}$. Furthermore, it is clear that future interpretations of 584 \AA observations of the local ISM must be cautious in drawing conclusions based on exact values of the solar 584 \AA flux without near-simultaneous full-disc measurements of that quantity.

The fact that our model fits were obtained with values of the ISM parameters generally similar to those recently used by other authors is significant in that most previous analysis of helium 584 \AA observations has been by means of a model strictly valid only for very low ISM temperatures. Our model does not possess this restriction, so the broad agreement of our analysis with those which preceded it reduces the possibility that the previously obtained fits of a low-temperature model to a high-temperature gas may have in some way been specious or misleading.

The low value of the number density of neutral helium in the local ISM, $0.0038 \pm 0.0021 \text{ cm}^{-3}$, is in conflict with early results derived from some of the first observations of ISM 584 \AA flux. Paresce, Bowyer, and Kumar

(1973a, b, 1974) gave $n_{\text{He}} = 0.032 \text{ cm}^{-3}$, and Weller and Meier (1974) stated that n_{He} was within the range $0.009-0.024 \text{ cm}^{-3}$. These early results depended the assumed value of F_{O} (as ours does), and the authors in question used values of that quantity approximately half the one we have chosen. Their value would be reduced by a factor of two if they had used our value for F_{O} .

The value of n_{He} which we report is consistent with more recent conclusions. Freeman et al. (1977) concluded $n_{\text{He}} \leq (0.004 \pm 0.0022) \text{ cm}^{-3}$ on the basis of observations made during the Apollo-Soyuz mission, with a different instrument. Fahr, Lay and Wulf-Mathies (1977) have reported data which support this conclusion. Given the nominal 0.085 relative cosmic abundance of helium atoms to hydrogen atoms (Allen 1973a), our value for n_{He} implies a number density n_{H} of neutral hydrogen in the nearby ISM of $0.045 \pm 0.025 \text{ cm}^{-3}$.

A value of n_{H} of 0.045 is a bit low to be consistent with the nominal 0.1 cm^{-3} obtained by 1216 Å observations of hydrogen in the local ISM (Fahr 1974). But as Fahr has pointed out, the interpretation of these observations is very model dependent, and there is considerable scatter in the reported values of n_{H} .

A value of n_H of 0.045 is consistent with hydrogen number densities determined from column density measurements within a few tens of parsecs. Table I lists densities obtained from 21 stars within 100 pc of the Sun, including 16 values consistent with column-averaged n_H at or below 0.05 cm^{-3} . In particular, Evans, Jordan and Wilson (1975) observed α CMi, at a distance of only 3.5 pc, and found n_H between 0.015 and 0.03 cm^{-3} . Perhaps, as Freeman et al. (1977) suggested, this region of very tenuous gas includes the solar system.

The preceding discussion suggests some possible conclusions about the structure and nature of the ISM near the Sun. McKee and Ostriker (1977) have recently developed a multiphase ISM model which explains the 10^5 - 10^6 K ISM temperatures inferred from interstellar O VI absorption lines (York 1974; Jenkins and Meloy 1974) by hot, tenuous gas in supernova remnants (also see Cox and Smith 1974), but which also allows for the presence of substantial volumes of partially ionized gas at temperatures near 8000 K, with neutral hydrogen number density near 0.09 cm^{-3} . This gas is produced by heating and ionization of small, cold interstellar clouds which are embedded in the hot

supernova remnants. Our results could be explained if the solar system lay within such a volume of gas. If so, then somewhere within a few pc of the Sun, one may find the cloud's cold core, with $T = 50-100$ K, $n_H = 10-100$ cm^{-3} , and radius $0.5-10$ pc (McKee and Ostriker 1977). In view of the small number of measured hydrogen column densities to nearby stars, it seems possible that a small cold cloud could have escaped detection even so close to the Sun as a few pc.

The clouds in the McKee-Ostriker theory are immersed in a network of old supernova remnants, some of which may have been reheated by more recent supernovae. Supernovae induce substantial long-lived bulk motions of interstellar material radially outward from their positions (Chevalier 1977 and references therein). On allowing for the motion of the Sun toward $\alpha = 271^\circ$, $\delta = +30^\circ$, at 19.7 km s^{-1} (Allen 1973b), we find that with respect to the local group of stars, the ISM approaches from $\alpha = 192^\circ$, $\delta = -67^\circ$, at 16 km s^{-1} , with uncertainties of about 15° and 3 km s^{-1} . These coordinates define a position within the Scorpius-Centarus association of early main-sequence stars, an association which might reasonably be expected to have

25

produced several supernovas earlier in its lifetime. The strong O VI absorption ($\log N_{\text{O VI}} = 12.96 \text{ cm}^{-2}$) reported by Jenkins and Meloy (1974) to β Cen A, at a distance of only 81 pc, may support the hypothesis of a nearby old supernova remnant.

Whatever the result of these conjectures, it is clear that observations of interstellar gas passing through the solar system can provide valuable insight into the structure and properties of the interstellar medium out to tens of parsecs from the Sun.

VII. ACKNOWLEDGMENTS

Robert Stern assisted with calibration and integration of the instrument. Numerous NASA personnel provided invaluable support during development, testing and flight. We particularly thank the NASA Project Scientist, T. R. Guili, for his assistance.

This research was supported by NASA contract NAS9-13807.

REFERENCES

- Adams, T. F., and Frisch, P. C., 1977. *Ap. J.*, 212, 300.
- Ajello, J. M., 1977, *Ap. J.*, preprint.
- Allen, C. W., 1973a, *Astrophysical Quantities* (3rd ed.; London: Althone Press), p. 30.
- _____, 1973b, *op. cit.*, p.252.
- Auer, L. H., and Shipman, H. L., 1977, *Ap. J. (Letters)*, 211, L103.
- Axford, W. I., 1972, *Solar Wind* (NASA SP-308), p. 609.
- Banks, P. M., and Kockarts, G., 1973, *Aeronomy, Part A*, Academic Press, New York and London, p. 157.
- Bertaux, J. L., and Blamont, J. E., 1971, *Astr. Ap.*, 4, 280.
- Bertaux, J. L., Blamont, J. E., Tabarie, N., Kurt, W. G., Bourgin, M. C., Smernov, A. S., and Dementeva, N. N., 1976, *Astr. Ap.*, 46, 19.
- Blum, P. W., and Fahr, H. J., 1970, *Astr. Ap.*, 4, 280.
- Bohlin, R. C., 1975, *Ap. J.*, 200, 402.
- Bohlin, R. C., Savage, B. D., and Drake, J. F., 1977, preprint.
- Bowyer, S., Freeman, J., Paresce, F., and Lampton, M., 1977, *Appl. Opt.*, 16, 756.
- Carlson, R. W., 1976, private communication.

Carruthers, G. R., and Page, T., 1972, Science, 177, 788.

Chevalier, R. A., 1977, Ann. Rev. Astron. Astrophys. 15, (Annual Reviews, Palo Alto), p. 175.

Cox, D. P., and Smith, B. W., 1974, Ap. J. (Letters), 189, L105.

Danby, J. M. A., and Camm, G. L., 1957, M.N.R.A.S., 117, 50.

Delaboudinière, J. P., and Crifo, J. F., 1975, paper presented at COSPAR meeting XVIII, Varna, Bulgaria, 1975 June 2.

Dupree, A. K., Baliunas, S. L., and Shipman, H. L., 1977, Ap. J., preprint.

Evans, R. G., Jordan, C., and Wilson, R., 1975, Nature, 253, 612.

Fahr, H. J., 1974, Space Sci. Rev., 15, 483.

Fahr, H. J., Lay, G., and Wulf-Mathies, C., 1977, paper presented at COSPAR meeting XX, Tel Aviv, Israel.

Freeman, J., and Paresce, F., 1978, Ap. J., (in the works)

Freeman, J., Paresce, F., Bowyer, S., and Lampton, M., 1976, Ap. J., 208, 747.

_____, 1978, J. Geophys. Res., (in the works)

Freeman, J., Paresce, F., Bowyer, S., Lampton, M., Stern, R., and Margon, B., 1977, Ap. J. (Letters), 215, L83.

Hall, L. A., and Hinteregger, H. E., 1970, J. Geophys. Res., 75, 6959.

Hall, L. A., Schweizer, W., and Hinteregger, H. E., 1965, J. Geophys. Res., 70, 105.

- Heroux, L., and Higgins, J. E., 1977, J. Geophys. Res., 82, 3307.
- Hinteregger, H. E., 1976, J. Atm. Terr. Phys., 38, 791.
- Holzer, J. E., and Axford, W. I., 1971, J. Geophys. Res., 76, 6965.
- Jacchia, L. G., 1971, Smithsonian Ap. Obs. Spec. Rept. No. 332.
- Jenkins, E. B., and Meloy, D. A., 1974, Ap. J. (Letters), 193, L121.
- Johnson, H. E., 1972, Planet. Space Sci., 20, 829.
- Lincoln, J. V., 1975, J. Geophys. Res., 80, 4773.
- Maloy, J. O., Carlson, R. W., Hartman, V. C., and Judge, D. W., 1975, paper presented at the 1975 Fall Annual Meeting of the American Geophysical Union, 1975 December.
- Margon, B., Lampton, M., Bowyer, S., Stern, R., and Paresce, F., 1976, Ap. J. (Letters), 210, L79.
- McClintock, W., Henry, R. C., Moos, H. W., and Linsky, J. L., 1976, Ap. J., (Letters), 204, L103.
- McClintock, W., Linsky, J. L., Henry, R. C., and Moos, H. W., 1975, Ap. J., 202, 165.
- McKee, C. F., and Ostriker, J. P., 1977, Ap. J., 218, 148.
- Meier, R. R., 1977, Astr. Ap., 55, 211.
- Moos, H. W., Linsky, J. L., Henry, R. C., and McClintock, W., 1974, Ap. J. (Letters), 188, L93.

Paresce, F., and Bowyer, S., 1973, Astr. Ap. 27, 1795.

Paresce, F., Bowyer, S., and Kumar, S., 1973a, Ap. J. (Letters), 183, L87.

_____, 1973b, J. Geophys. Res., 78, 71.

_____, 1974, Ap. J., 187, 633.

Rogerson, J. B., York, D. G., Drake, J. F., Jenkins, E. B., Morton, D. C.,
and Spitzer, L., 1973, Ap. J. (Letters), 181, L110.

Rusch, D. W., Torr, D. G., Hays, P. B., and Torr, M. R., 1976, Geophys.
Res. Letters, 9, 537.

Thomas, G. E., and Krassa, R. F., 1971, Astr. Ap. 11, 218.

Wallis, M. K., 1973, Ap. and Space Sci., 20, 3.

_____, 1974, M.N.R.A.S., 167, 103.

_____, 1975, Planet. and Space Sci., 23, 419.

Weller, C. S., and Meier, R. R., 1974, Ap. J., 193, 471.

York, D. G., 1974, Ap. J. (Letters), 193, L127.

_____, 1976, Ap. J., 204, 750.

TABLE I

Star	Distance (pc)	$n_{\text{HI}} (\text{cm}^{-3})$	Reference for Column Density of HI
α Cen	1.34	0.20 ± 0.05	Dupree et al. (1977)
ε Eri	3.3	< 0.12	McClintock et al. (1976)
α CMi	3.5	$0.015 - 0.030$	Evans et al. (1975)
β Gem	10.7	< 0.15	McClintock et al. (1975)
α Boo	11.1	< 0.1	Moos et al. (1974)
α Aur	14	0.03 ± 0.01	Dupree et al. (1977)
α Tau	20.8	< 0.2	McClintock et al. (1975)
α Leo	22	0.02	Rogerson et al. (1973)
σ Eri	28	0.07	Rogerson et al. (1973)
α Gru	29	$0.09 - 0.18$	York (1976)
η UMa	42	0.005	York (1976)
σ Sgr	57	< 0.17	Bohlin et al. (1977)
HZ 43	62.5	< 0.013	Auer et al. (1977)
α Pav	63	< 0.01	Bohlin et al. (1975)
α Sgr	80	< 0.12	Bohlin et al. (1975)
β Cen	81	0.13	Bohlin et al. (1977)
β Lib	83	$0.06 - 0.13$	York (1976)
ζ Cen	83	< 0.39	Bohlin et al. (1977)
α Vir	87	0.037	Bohlin et al. (1977)
Feige 24	90	< 0.011	Margon et al. (1976)
λ Sco	100	< 0.078	Bohlin et al. (1977)

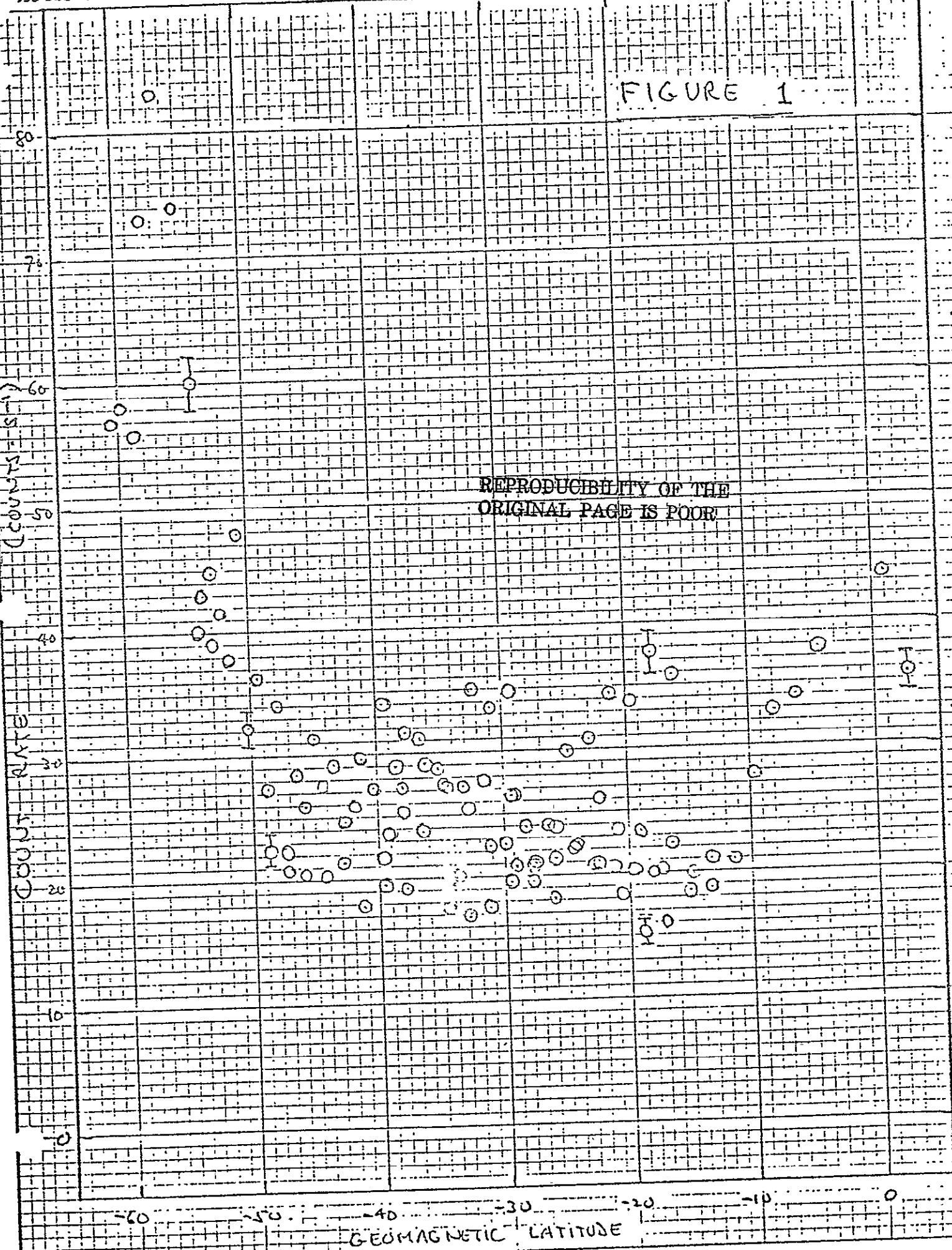
FIGURE CAPTIONS

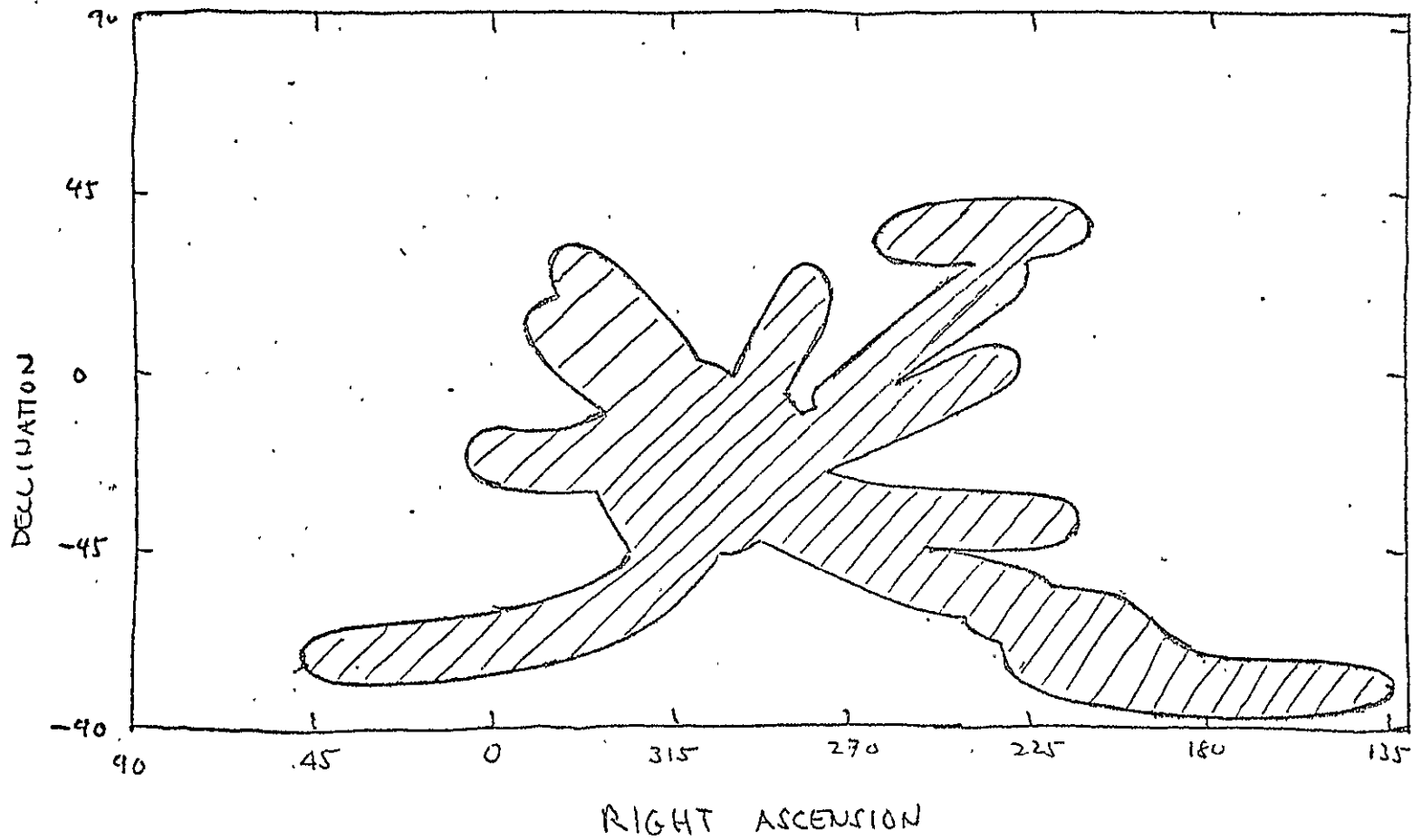
Figure 1: Observed cell-empty count rate, corrected for atmospheric absorption, as a function of magnetic latitude. Representative error bars are shown.

Figure 2: The celestial sphere, indicating by hatching the portions surveyed by the Apollo-Soyuz helium 584 Å photometer, while gathering the 42 minutes of data analyzed herein.

Figures 3 & 4: Reduced observed fluxes and model predictions for the eight discrete intervals of data collection. Open circles = cell-empty fluxes; Solid circles = cell-full fluxes. Representative error bars are shown. Shaded area = envelope of model predictions as temperature varies from 5000 to 20,000 K. The model predictions have been adjusted so that the product $n_{\text{He}} F_{\text{O}} = A \times 10^{-7}$ photons $\text{cm}^{-5} \text{s}^{-1}$, where the value of A is displayed at the bottom of each panel. All fluxes are in rayleighs, and each data point represents one 30-s bin.

FIGURE 1





REPRODUCIBILITY OF THE
ORIGINAL PAGE IS POOR.

Figure 2

FIGURE 3

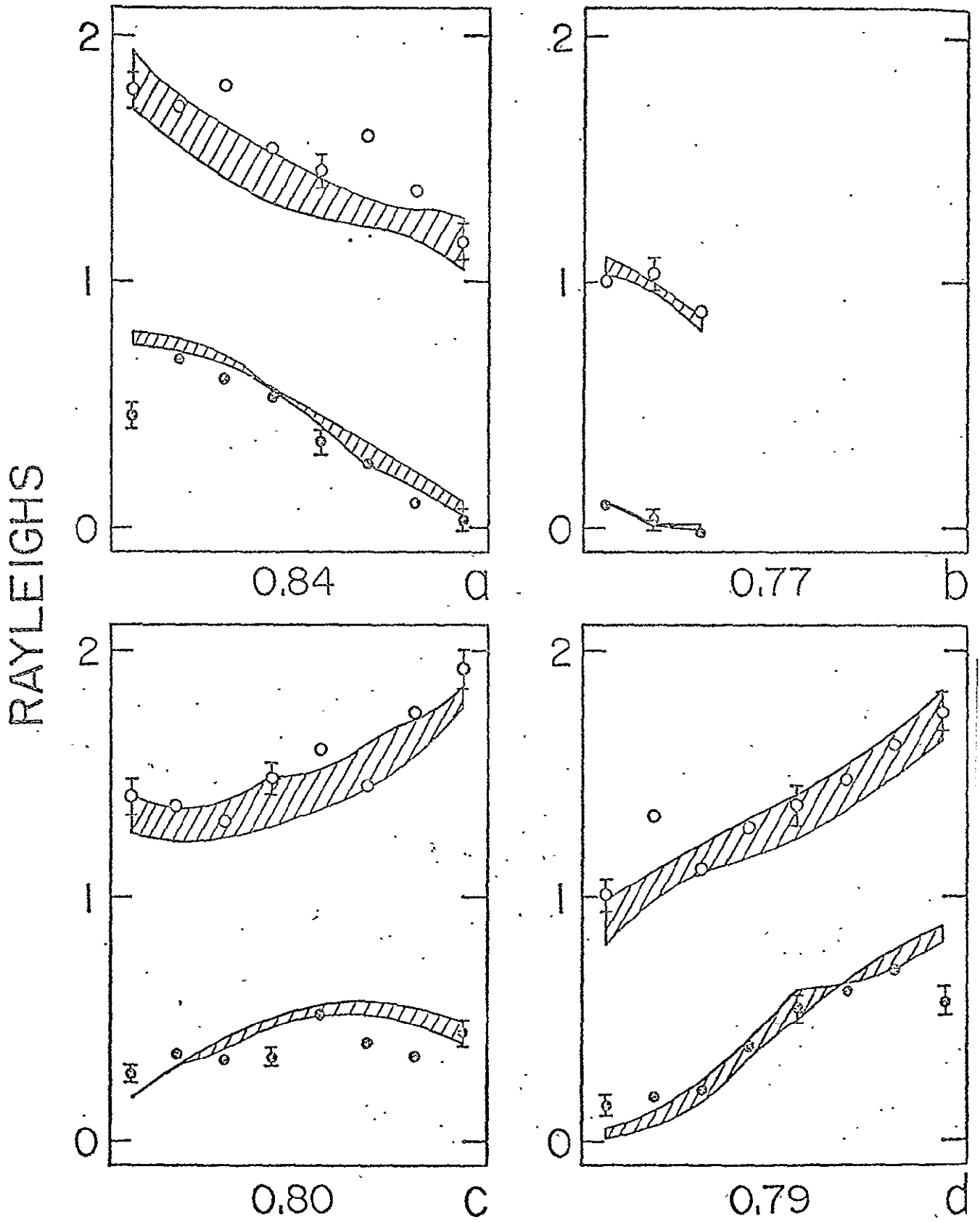
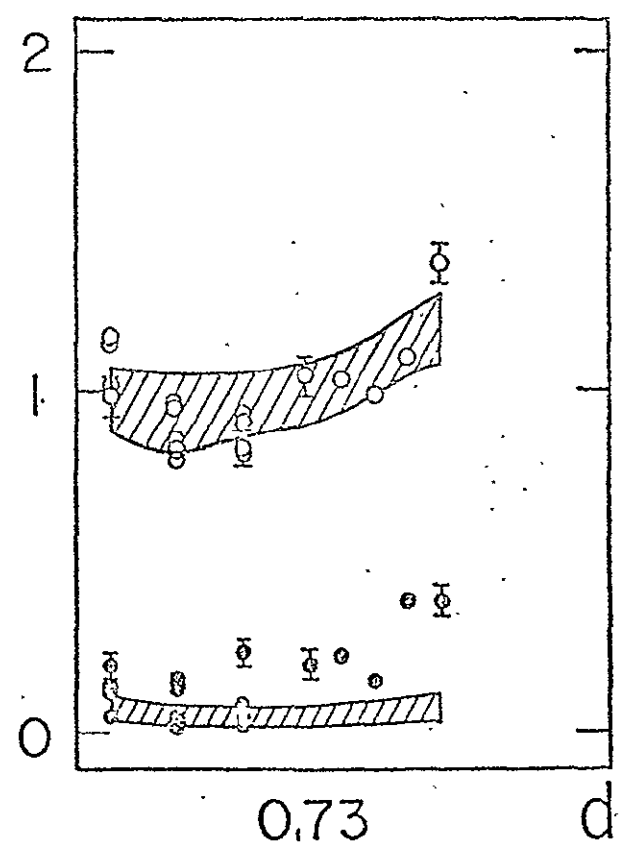
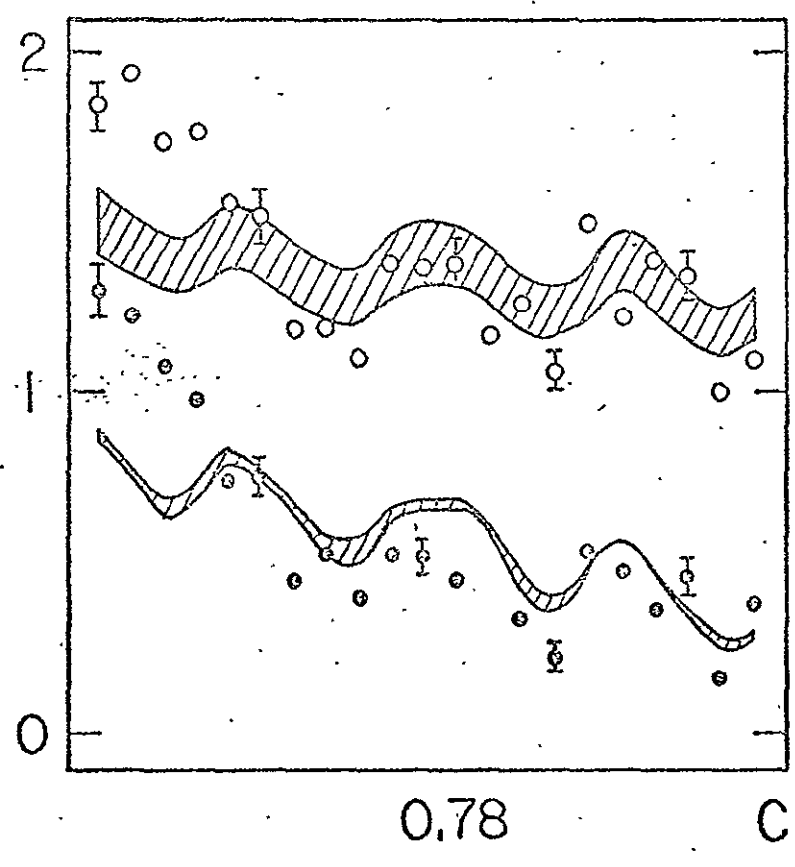
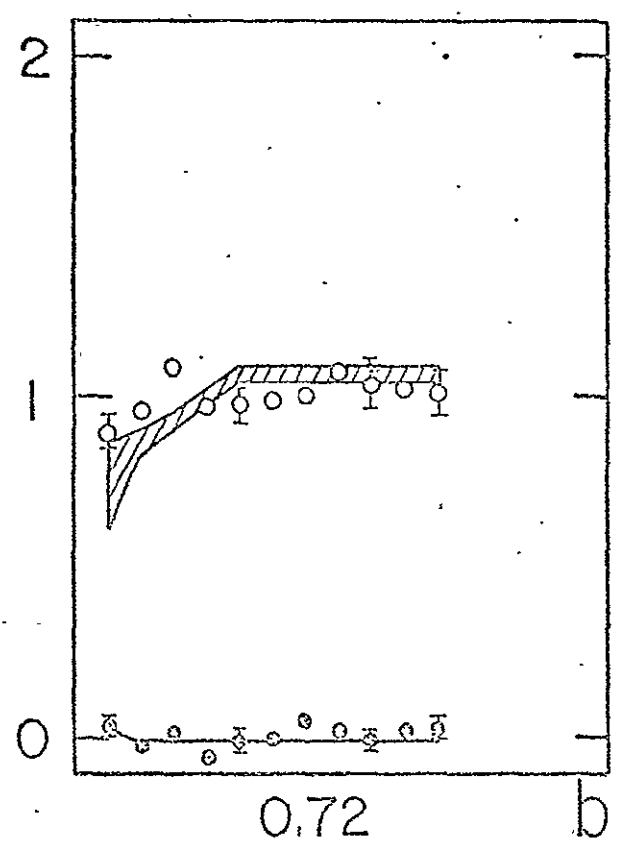
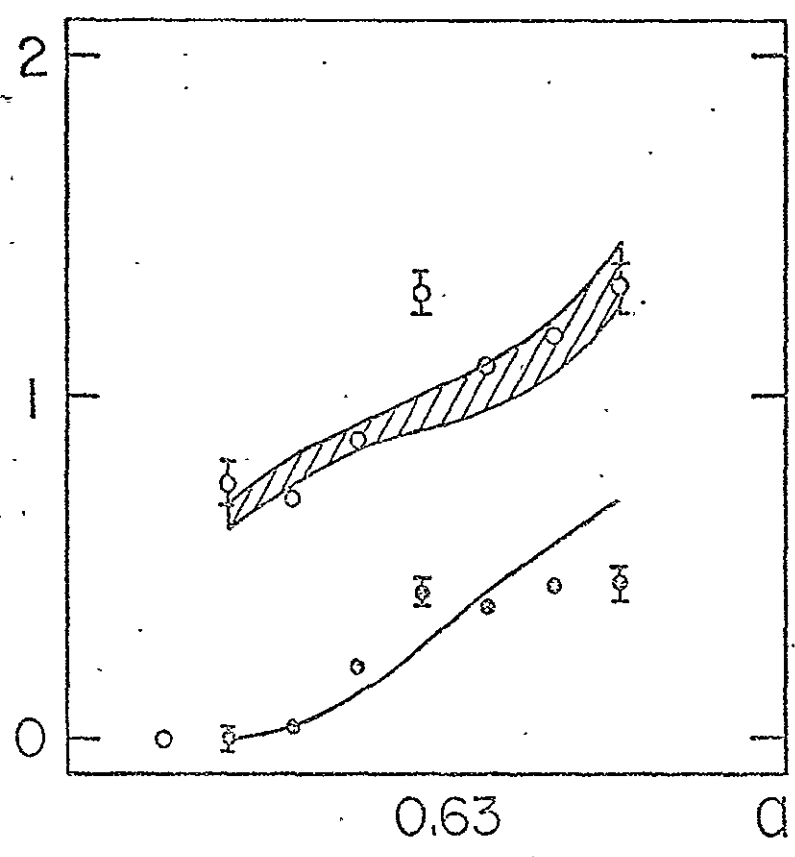


FIGURE 4

KAYLEIGHTS



EXTREME ULTRAVIOLET DAYGLOW OBSERVATIONS

WITH A

HELIUM GAS ABSORPTION CELL

Jay Freeman, Francesco Paresce,
Stuart Bowyer, and Michael Lampton

ABSTRACT

During the Apollo-Soyuz Test Project, an extreme-ultraviolet photometer with a cyclically operated helium gas absorption cell observed the daytime sky from an orbital altitude of 225 km. When the line of sight pointed more than 60° from the sun, the instrument detected 2 to 70 rayleighs of flux scattered from neutral geocoronal helium at wavelengths from 504 to 584 Å. The instrument also detected other radiation in the band 500-700 Å of similar spatial distribution to the helium flux, which was definitely not due to the He I 584 Å spectral line. Possible sources of this radiation are discussed.

INTRODUCTION

The extreme ultraviolet (EUV) dayglow between 100 and 1000 Å has been observed by a number of authors (Donahue and Kumer 1971; Meier and Weller 1972, 1974; Carruthers and Page 1972, 1976; Kumar, Bowyer and Lampton 1973; Carlson and Judge 1973). Fluxes of several rayleighs to several thousand rayleighs have been detected and ascribed to specific spectral lines. However, poor EUV spectral resolution, in part due to the relatively broad band passes of available EUV filters, has made wavelength identification difficult and may possibly have prevented the isolation of closely-spaced lines. A spectrometer measurement (Christensen 1976) provided 20 Å resolution between 550 and 1250 Å, which is still inadequate to separate many possible dayglow lines.

We have recently flown a photometer sensitive at 500-700 Å, in which a helium gas resonance absorption cell permits separation of the 584 Å He I flux from other radiation in this band. The observation allows confirmation of the coarse-resolution spectrometer measurements of 584 Å flux just discussed, and permits study of the spatial distribution of both the 584 Å flux and of other, unresolved radiation in the band.

INSTRUMENTATION

The Apollo-Soyuz helium glow detector has been described in detail by Bowyer et al. (1977). In brief, it contained four EUV photometers, each with a 13 mm diameter active area and a 14° FWHM circular field of view. One photometer consisted of a channel electron multiplier with a helium gas resonant absorption cell which was equipped with one tin and one aluminum thin metallic film. The EUV bandpass of the instrument was defined by these films, which formed the entrance and exit apertures of the absorption cell and transmitted from about 500 Å to about 700 Å. This bandpass contained all neutral helium ground-state resonance lines, from the $1s^2-1s2p$ transition at 584 Å to the continuum edge at 504 Å. The cell was alternately evacuated and filled with helium at a pressure of 1.4 torr, with a helium column density of 4.4×10^{17} atoms cm^{-2} . The filled cell superimposed on the 584 Å line an absorption feature of 100 mÅ FWHM, which absorbed more than 99 percent of incident radiation over a band 40 mÅ wide. A narrower absorption feature was superimposed on each shorter wavelength ground-state helium line. Every 0.1 s the number of counts detected was telemetered, together with the helium cell pressure and other information.

The instrument was calibrated in the laboratory before flight using a hollow-cathode discharge lamp operated with various gases to yield radiation in the 200 to 2000 Å region. An NBS-calibrated Al₂O₃ windowless photodiode was used as a reference standard. The measured photometric efficiency of the instrument, versus wavelength, is shown in Figure 1. The overall sensitivity of the detector to diffuse 584 Å flux was 18 ± 3.6 counts s⁻¹ rayleigh⁻¹. The detector response was constant as long as its photosensitive surface was directly illuminated by the calibration beam. When the beam reached the detector after one or more reflections from surfaces adjacent to the optical path, the response was reduced by a factor of 200 or more. When the instrument viewed a diffuse homogeneous source of EUV radiation to which it was sensitive, less than three per cent of the photons detected reached the photosensitive surface by such reflections.

DATA REDUCTION

We imposed several constraints on the data selected for analysis and discussion here. We required that the line of sight point within 97° of the local zenith, which corresponds to the lower edge of the field of view being tangent to the Earth's limb. We excluded data taken in or near the South Atlantic Anomaly. To avoid contamination by sunlight reflected from the spacecraft, we included only data taken when the line of sight pointed more than 60° from the Sun. These conditions were met by a total of 1105s of data, all taken on July 20 or 21, 1975, from an orbital altitude of about 225 km.

We binned all data into consecutive 5-s intervals, each containing approximately equal times with the gas absorption cell filled and evacuated. The set of 0.1-s telemetered data samples in each bin was filtered to eliminate any anomalously high or low count rates, such as might be caused by electrical noise or telemetry dropouts. In this process, each 0.1-s count-rate sample was examined to see whether it lay within three standard deviations of the mean of all other samples in that bin. If not, it was discarded. The filtering was repeated until no samples were discarded in a complete successive examination of all samples remaining in the bin in question. The number of samples eliminated was less than five per cent, and was consistent with the number expected from Poisson statistics.

With the gas absorption cell empty, the count rates detected ranged from 81 to 3446 counts s^{-1} . With the cell filled, the corresponding range of rates was 12 to 2662 counts s^{-1} . We correlated the reduced cell-full and cell-empty data with several parameters upon which airglow intensities might depend, including solar zenith angle, line-of-sight elevation, and angle between line of sight and the Sun.

The only correlation we found was with solar zenith angle, which is also the angle in arc on the Earth's surface between the subsolar point and the spacecraft position. In Figure 2 we show the cell-empty and cell-full count rates plotted against solar zenith angle. Statistical count-rate errors are comparable to the size of the dots plotted. The straight lines are linear regression fits for the two cases. This dependence of the observed fluxes on spacecraft position is qualitatively consistent with the model of He I 584 Å scattering from an optically thick neutral helium geocorona developed by Meier and Weller (1972).

As shown in Figure 2, the cell-full count rate tracked the cell-empty count rate remarkably well. Although the fluxes observed varied by an overall factor of twenty, the cell-full count rate remained at about 0.3 of the cell-empty count rate throughout.

DISCUSSION AND CONCLUSIONS

The gas absorption cell was designed to absorb all 584 Å radiation scattered from the Earth's geocorona, even when that radiation was Doppler-shifted by the 8 km s^{-1} speed of an orbiting spacecraft. A nominal thermosphere temperature of 1000°K (Jacchia 1971) corresponds to thermal-Doppler broadening of the scattered 584 Å line to 3 mÅ FWHM, and an additional 8 km s^{-1} speed along the line of sight corresponds to a further Doppler shift of about 16 mÅ. Thus even if the instrument line of sight pointed parallel to the orbital motion, the geocoronal helium line would have been completely absorbed. For most of the data discussed here, the component of orbital velocity along the line of sight was substantially less than 8 km s^{-1} . The temperatures necessary to thermal-Doppler broaden the geocoronal 584 Å line to a FWHM comparable to the 99 per cent absorption width of the gas cell, are at least an order of magnitude greater than the 1000°K heretofore assumed. We are therefore confident that the helium glow detector gas absorption cell did in fact absorb all geocoronal 584 Å radiation.

Radiation at wavelength below the helium continuum edge at 504 Å would also be in part absorbed by the gas cell, with the absorption cross-section varying in proportion to wavelength cubed. We do not believe such radiation could have contributed appreciably to either the cell-full or cell-empty fluxes.

We are not aware of any reports of dayglow measurements from 300 to 504 Å other than broadband photometer studies. However, the solar EUV spectrum (Timothy 1976, Hinteregger 1976) shows only one strong line in that range likely to be scattered resonantly by atmospheric species. That line is the ground state He II transition at 304 Å.

Kumar, Bowyer and Lampton (1973) measured 304 Å dayglow flux with a photometer from altitudes of 120 to 190 km, at a solar zenith angle of 42°, and after correction for atmospheric absorption found an overhead flux of 15 rayleighs. This flux would cause our instrument to count at less than 10 counts s⁻¹, which is negligible compared to nearly all of our data.

Schmidtke (1976) gives a total solar He I continuum flux comparable to the 584 Å line emission: that is, about 10⁹ photons cm⁻² s⁻¹. Standard atmospheric models (Jacchia 1971) indicate approximately 10¹⁴ - 10¹⁵ neutral helium atoms per square centimeter above 220 km. Hence, assuming a nominal absorption cross-section of 2 x 10⁻¹⁸ cm², the instrument would observe 0.2 - 2 rayleigh of atmospheric emission near the neutral helium continuum edge, caused by helium photoionization due to the solar continuum and subsequent recombination.

As shown in Figure 1, the instrument sensitivity falls rapidly below 550 Å, so that two rayleighs of flux at 500 Å could cause at most a few counts per second. The maximum observed cell-full flux, as shown in Figure 2, was more than two orders of magnitude greater.

Both theoretical work (Freeman and Paresce 1978, and references discussed therein) and experimental results (Freeman et al. 1978, and references therein) indicate that the total solar 584 Å flux scattered from the interstellar medium passing through the solar system is no more than a

few rayleighs for the view directions under consideration here. This flux is also much too small to explain our observations.

The preceding analysis leads to three conclusions. First, by subtracting cell-full from cell-empty count rates, we conclude that the daytime He I EUV geocoronal flux intensity spans the range 2 - 70 rayleighs. This value compares favorably with the 25 rayleighs of 584 Å flux reported by Christensen (1976) between 210 and 240 km at a solar zenith angle of 74°. If the 304 Å line is in fact the only strong day-glow line from 300 to 504 Å, then our measurement is not contaminated by any radiation whose wavelength differs from He I ground-state lines by more than a few mÅ.

Second, inasmuch as the gas cell was designed to absorb all geocoronal 584 Å flux, the substantial 500-700 Å flux observed through the filled cell must have some other origin. Interplanetary 584 Å flux might be Doppler-shifted sufficiently to be transmitted by the gas cell, but the theoretical work cited indicates that this flux is much too weak to explain our cell-full data. We cannot calculate an absolute intensity for this radiation, since its wavelength or wavelengths, and hence the correct calibration factors for our detector, are not known.

Third, the strong correlation between the cell-full flux and such a local parameter as spacecraft position, suggests that this flux originated

near the Earth. The intensity of this radiation varies with the observer's position in a manner similar to that of the 584 Å flux, at least for the range of observation positions and directions considered here.

Kumar, Bowyer and Lampton (1973) have reported detection of dayglow flux other than at 584 Å, within the band 500-800 Å. Carruthers and Page (1972, 1976) and Christensen (1976) have reported possible detections of dayglow spectral lines between 600 and 700 Å with intensities comparable to He I 584 Å. Delaboundinière (1977) has calculated theoretical emission rates for O II dayglow lines at 537 and 581 Å, at a solar zenith angle of 0°, and predicts fluxes of 100-200 rayleighs at the altitudes from which we observed. Any of these results might explain our cell-full fluxes. More detailed investigations with high-resolution spectrometers will be needed to define conclusively the spectral distribution of the dayglow radiation in this band.

ACKNOWLEDGMENTS

We thank Robert Stern for assistance with instrument testing and integration, and Bruce Margon for assistance with ground operations during flight. This research was supported by NASA contract NAS9-13807.

FIGURE CAPTIONS

Figure 1: Measured end-to-end photometric efficiency of photometer, extrapolated between data points, with typical error bars.

Figure 2: Cell-full (lower) and cell-empty (upper) count rates versus solar zenith angle. Calculated linear regressions fits shown by diagonal lines. Typical error bars are given. Five points above 2200 counts sec⁻¹ are not shown.

REFERENCES

- Bowyer, S., Freeman, J., Paresce, F., Lampton, M., Stern, R., and Margon, B., Extreme ultraviolet photometer for observations of helium in interplanetary space, *Appl. Opt.*, 16, 756, 1977.
- Carlson, R. W., and Judge, D. L., Rocket observations of the extreme ultraviolet dayglow, *Planet. Space Sci.*, 21, 879, 1973.
- Carruthers, G. R., and Page, T., Apollo 16 far ultraviolet camera/spectrograph: Earth observations, *Science*, 177, 788, 1972.
- _____, Apollo 16 far ultraviolet spectra of the terrestrial airglow, *J. Geophys. Res.*, 81, 1683, 1976.
- Christensen, A. B., A rocket measurement of the extreme ultraviolet dayglow, *Geophys. Res. Lett.*, 3, 221, 1976.
- Delaboudinière, J. P., Possible contribution of radiation from the $2s2p^4\ ^2P$ level of O II in dayglow measurements of the He I line at 584 Å, *Planet. Space Sci.*, 25, 193, 1977.
- Donahue, T. M., and Kumer, J. B., An observation of the helium I 584 Å dayglow radiation between 400 and 1000 km, *J. Geophys. Res.*, 76, 145, 1971.
- Freeman, J., and Paresce, F., accepted for publication, *Astrophys. J.*, Sept. 1978.
- Freeman, J., Paresce, F., Bowyer, S., and Lampton, M., in preparation, 1978.
- Hinteregger, H. E., EUV fluxes in the solar spectrum below 2000 Å, *J. Atm. Terr. Phys.*, 38, 791, 1976.
- Jacchia, L. G., *Smithsonian Ap. Obs. Spec. Rept. No. 332*, 1971.
- Kumar, S., Bowyer, S., and Lampton, M., Observations of the helium II 304-Å and helium I 584-Å atmospheric dayglow radiation, *J. Geophys. Res.*, 78, 1107, 1973.
- Meier, R. R., and Weller, C. S., EUV resonance radiation from helium atoms and ions in the geocorona, *J. Geophys. Res.*, 77, 1190, 1972.
- _____, Extreme ultraviolet observations of the latitudinal variation of helium, *J. Geophys. Res.*, 79, 1575, 1974.
- Schmidtke, G., EUV indices for solar-terrestrial relations, *Geophys. Res. Lett.*, 3, 573, 1976.
- Timothy, J. G., Measurements of the solar spectral irradiance between 300 Å and 1200 Å, review paper for NASA workshop on the Physical Output of the Sun, 1976. Preprint, Center for Astrophysics, Cambridge, MA, 1976.

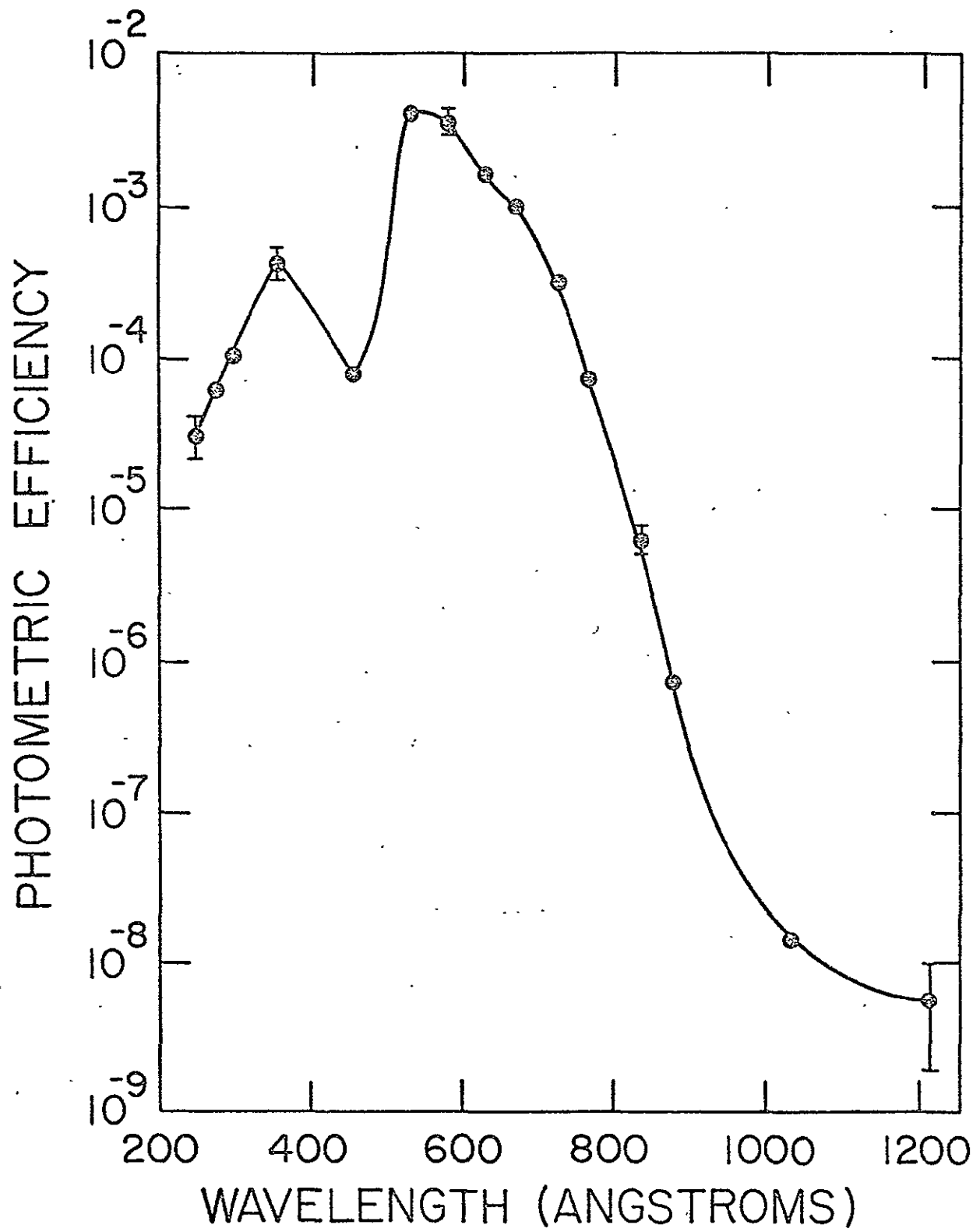


Figure 1.

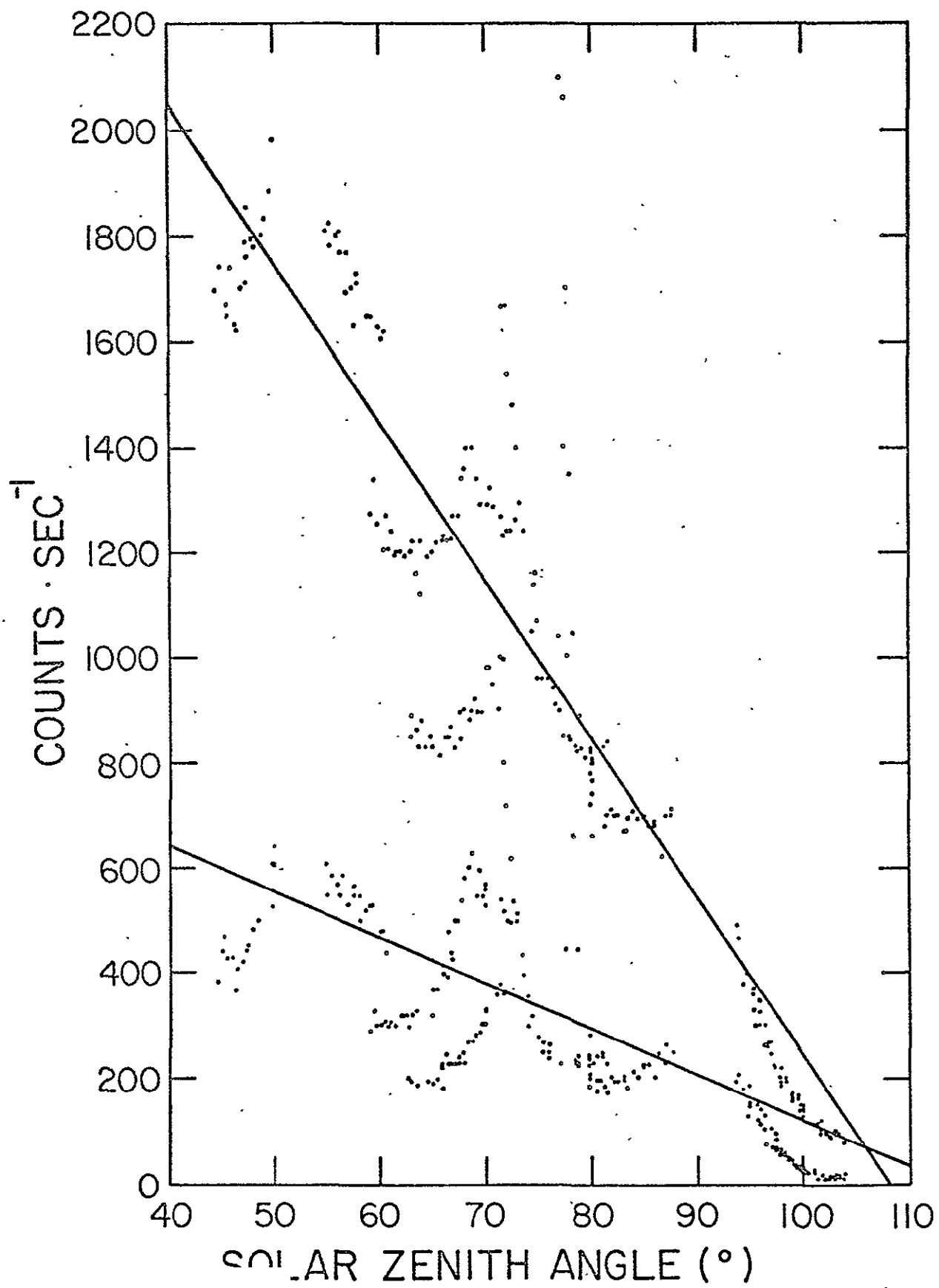


Figure 2.

SPACE SCIENCES LABORATORY

EUV SCATTERING FROM LOCAL INTERSTELLAR HELIUM AT NONZERO TEMPERATURE:
IMPLICATIONS FOR THE DERIVATION OF ISM PARAMETERS

Jay Freeman and Francesco Paresce

March 1978

UNIVERSITY OF CALIFORNIA, BERKELEY

ABSTRACT

We have developed a model for resonant scattering of solar extreme ultraviolet light from atoms of the local interstellar helium passing through the solar system, which is valid even if the interstellar gas is hot. The model features numerical integration of the phase-space number density function of Danby and Camm (1975). We compare this model with the modified cold-gas model widely used previously, for values of the model parameters presently believed to be nominally correct for 584 Å scattering from neutral helium. The new model predicts significantly different observed patterns of scattered flux than the old one. The new model predicts substantial variations of observed flux with temperature, in circumstances in which the old model predicts no variation at all. The modified cold-gas model is invalid for analysis of helium observations whose field of view lies near the downstream symmetry axis of the gas motion, and for the determination of the temperature of the distant gas. It may be of limited use for other observations, for analyses which depend only on the relative intensities of flux observed from different parts of the sky. Much previous work must be reexamined in light of these new constraints.

INTRODUCTION

The nearby interstellar medium (ISM) may be directly observed from a rocket or spacecraft by solar extreme ultraviolet (EUV) light resonantly scattered from its constituent gas atoms. During the last fifteen years, a number of authors (see Fahr 1974, Bertaux et al., 1976, and Freeman et al., 1976a, and references cited therein) have made such observations, either of hydrogen at 1216 Å or of neutral helium at 584 Å, and have attempted to deduce from them properties of the nearby ISM. Several of these quantities, notably temperature and number density, are difficult to obtain by other means.

There are no closed formulae whereby these properties may be directly calculated by simple substitution of the observed data. All analysis has been by model fitting. In these models, the intensity I of resonantly scattered flux which is seen by an observer with a specified line of sight is expressed as an integral:

$$(1) \quad I = \int n(\vec{v}, s) F(v_*, s) a(v_*, \vec{v}, v_i) p(\theta(s)) d^3\vec{v} dv_* dv_i ds$$

In this equation, s is path length along the line of sight, \vec{v} is gas atom velocity at the point s, v_* is photon frequency in an inertial frame attached to the Sun, and v_i is the photon frequency in an inertial frame attached to the observer. The function $n(\vec{v}, s)$ is the phase-space number density of scattering atoms at s, $a(v_*, \vec{v}, v_i)$ is the cross-section for atoms of velocity \vec{v} to scatter solar photons of frequency v_* toward the observer with frequency v_i ; $\theta(s)$ is the angle between the Sun, the point s,

and the observer, $p(\theta(s))$ is a phase function, and $F(v_*, s)$ is the solar EUV intensity at s . In practice, equation (1) must also include the sensitivity of the observing instrument as a factor, and if that sensitivity varies significantly over the breadth of the resonant line in question, it must appear within the integral. Integrals of this form have been described in greater detail in Fahr (1974), Bertaux *et al.* (1976), Freeman *et al.* (1976a), and in references cited therein,

Within equation (1), the forms of a and p are well-known from atomic physics, and F is generally described by a Gaussian of given FWHM and intensity, but the proper evaluation of the phase-space number density $n(\vec{v}, s)$ has posed substantial theoretical and numerical difficulties. This function has often been replaced by an approximation derived from the so-called cold model, in which the thermal speeds of individual gas atoms are assumed to be small compared to the bulk speed V_B of the distant ISM. When a first-order correction for thermal speeds which are not small compared to the bulk speed is applied to the region downstream from the Sun with respect to the approaching ISM (Feldman, Goldstein and Sherb 1972; Blum, Pfleiderer and Wulf-Mathies 1975), the model is called the modified cold model. It has been used to analyze most data so far published. We shall now demonstrate that for analysis of helium observations, the modified cold model is wrong by significant amounts in many cases of interest.

THE MODIFIED COLD MODEL

The cold model phase-space density function derives from the assumption that the distant ISM has a temperature of zero; that is, that all atoms

move in the same direction with the same speed. Given a point near the Sun, not located on the axis of symmetry, it can be shown that only two orbits with the zero-temperature initial conditions cross that point. The number density function is as given, for example, by Blum, Pfleiderer and Wulf-Mathies (1975), equations (4) and (17),

If the selected point is directly upstream of the Sun only one orbit crosses it, but in the zero-temperature approximation every orbit crosses the downstream symmetry axis. This latter condition leads to an unphysical density spike at the downstream axis, and the cold model thereby falsely predicts a bright, localized EUV flux scattered from that region. Feldman, Goldstein and Sherb (1972) and Blum, Pfleiderer and Wulf-Mathies (1975) have published formulae for altering the number density function close to the downstream axis to take first-order account of non-zero atomic thermal speeds. With the addition of such formulae, the cold model becomes the modified cold model.

In this model, the three-dimensional integral over gas velocity in equation (1) collapses to a two-term sum, and Dirac delta functions in $a(v_*, \vec{v}, v_i)$ allow the integrations on v_* and v_i to be performed immediately. The evaluation of the flux I in this model is thereby reduced to a one-dimensional numerical integration along the line of sight, which can be accomplished quickly on even a small computer.

A HOT MODEL

The distant ISM is better described, however, by a Maxwell-Boltzmann distribution of temperature T, moving with bulk speed V_B in a certain direction,

This initial condition makes the analytical description of the phase-space number density function $n(\vec{v}, s)$ a much more difficult problem. Furthermore, the use of such numerical techniques as Monte Carlo methods to evaluate $n(\vec{v}, s)$, requires large amounts of time on even the fastest of present-day computers. It is therefore not surprising that most workers in the study of the local ISM continued to use the modified cold model, even when early results indicated that thermal speeds might in fact not be small.

In 1975 Wallis pointed out that an analytic solution for $n(\vec{v}, s)$ under the initial conditions just given had been obtained by Danby and Camm in 1957, in the context of a different astrophysical problem. The Danby and Camm expression for $n(\vec{v}, s)$ contains an exponential of a complicated trigonometric function which is difficult to manipulate analytically. Furthermore, although Dirac delta functions in $a(v_*, \vec{v}, v_i)$ allow two of the integrations in equation (1) to be performed immediately, the calculation of an observed flux using the Danby and Camm $n(\vec{v}, s)$ nevertheless requires a four-dimensional integration, three dimensions more than with the modified cold model.

We have developed a program to evaluate equation (1) by numerical integration, using the Danby and Camm number density function, modified by the inclusion of the factor $\exp(-\beta_0 r_E^2 \theta / V_B p)$ which was used by preceding authors (e.g. Blum, Pfleiderer and Wulf-Mathies 1975) to allow for the loss of gas atoms by ionization due to solar EUV. In this factor, β_0 is the rate at which gas atoms are ionized at one astronomical unit r_E from the Sun, θ is the angle through which a gas atom has orbited about the Sun, and

p is the impact parameter of the orbit in question. We refer to this model as the hot model. Meier has developed a similar model, also using the Danby and Camm number density, and has published a description of some of the features of its predictions (Meier 1977). Unfortunately, his published results so far include only a small number of observer positions and lines of sight, and make no direct comparison with the cold model,

Our hot model uses Simpson's rule to perform all four integrations. In testing the program, we varied the number and spacing of points at which the integrand was evaluated, until we observed an apparent asymptotic limit to the calculated value of the flux I . For all further work, we used a number and spacing of points which produced a value of I within ten per cent of the observed limit.

We checked the program validity by using several limiting cases singly and in combination. At $T = 0$, the hot model predictions should equal the modified cold model predictions. Since both our computer codes use the expression $1/T$ repeatedly, we could not simply substitute $T = 0$ in the program. Instead, we set all other parameters at nominal values and compared the predictions of our two models as T was reduced by increments to values as low as 300 °K. At these low temperatures, for most lines of sight, the models agreed to within about ten per cent, which is the empirically determined accuracy of the numerical integration routines used. For lines of sight close to the downwind symmetry axis the disagreement at low temperature was much greater. Inasmuch as the analytic forms of both models predict divergent atomic number densities on the downwind axis as T approaches zero, this result is not surprising. Our programs were designed with substantially higher temperatures in mind.

We also evaluated the hot model in several other limiting cases in which some of its features can be checked against analytic expressions. For example, with solar mass and radiation pressure set equal to zero, and with solar 584 Å line width very large compared to the Doppler shift caused by helium thermal speeds, the hot model predicted an observed line whose Gaussian profile matched that calculated from the Maxwell-Boltzmann distribution of the distant gas. The center of this line was Doppler-shifted by the radial velocity between the gas and the observer.

Calculations using the hot model also displayed the various symmetries imposed by the geometrical symmetries of the physical problem.

The program provides the total observed flux and the observed line profile. It has provision for also calculating the flux and line profile observed when a helium gas absorption cell (Freeman et al., 1976b; Bowyer et al., 1977; Fahr et al., 1977) is interposed between the observer and the line of sight. We have so far used the program only to investigate the behavior of neutral helium as observed via the resonant scattering of solar EUV at 584 Å. Each evaluation of the integral (1) requires three to fifteen minutes of central processor time on a CDC 6400 computer.

MODEL PARAMETERS

Fourteen physical parameters determine the predictions of the models. These are three parameters describing the bulk velocity of the distant gas, the distant gas temperature T and neutral helium number density n_{∞} , the rate β_0 at which the gas is ionized at one A.U. from the Sun, the FWHM $\Delta\lambda$ of the solar resonance line, the solar line flux F_0 at one A.U. from the Sun, the ratio μ of the pressure of light to the force of solar gravity on a gas atom, three parameters characterizing the position of the observer and two describing the line of sight (LOS) of the observation,

In order to reduce the amount of calculation required to compare the models, we restricted several of these parameters to values or narrow ranges near the values presently believed correct, or to values commonly used in previous work.

We assumed that the distant ISM moves toward the direction $\alpha = 72^\circ$, $\delta = +15^\circ$, first given by Weller and Meier (1974) and later confirmed by Bertaux et al. (1976). Both models are exactly linear in both n_∞ and F_0 , so that the exact values selected for these parameters alter the predictions only by an overall scale factor. We selected $n_\infty = 0.01 \text{ cm}^{-3}$ and $F_0 = 10^9 \text{ cm}^{-2} \cdot \text{s}^{-1}$, which are numerically convenient values near the ranges recently reported. (Paresce, Bowyer and Kumar 1973, 1974; Weller and Meier 1974; Freeman et al., 1977). We assumed $\beta_0 = 6,8 \times 10^{-8} \text{ s}^{-1}$ and $\Delta\lambda = 0,12 \text{ \AA}$. These values are within the ranges reported in recent studies of solar properties (Delaboudinière and Crifo 1975; Doschek, Behring and Feldman 1974; Milkey, Heasley and Beebe 1973; Banks and Kockarts 1973). We assumed $\mu = 0$ throughout. We considered only observers along the Earth's orbit, and in general constrained the LOS to the celestial hemisphere opposite the Sun.

RESULTS

Downwind Sky Map. In Figures 1 and 2 we show maps of 584 \AA skyglow predicted respectively by the modified cold model and hot model, for an observer at the point on the Earth's orbit that is closest (7 degrees of arc) to the downwind symmetry axis of the gas motion, for distant gas bulk speed $20 \text{ km} \cdot \text{s}^{-1}$ and temperature 10^4 K . Several different kinds of observations (Bertaux et al. 1976; Freeman et al. 1976a; Adams and Frisch 1977) indicate that V_B is in fact within a few $\text{km} \cdot \text{s}^{-1}$ of 20. A temperature of 10^4 K is the approximate mid-point of the range of gas temperatures determined by recent

authors (Paresce, Bowyer and Kumar 1973, 1974; Weller and Meier 1974; Bertaux et al. 1976). The maps are symmetric about the line $\alpha = 72^\circ$. The isophotes for 584 Å flux levels in rayleighs are interpolated between specific predictions spaced at most 22.5 degrees of arc apart.

Both models predict a pronounced maximum in intensity near the downstream direction $\alpha = 72^\circ$, $\delta = +15^\circ$, due to the focusing effect of solar gravity. The maximum predicted by the modified cold model is more sharply defined than the one predicted by the hot model. Furthermore, the modified cold model predictions plotted span a greater range than the hot model predictions. On the modified cold model map, the highest flux predicted is slightly more than twice as great as the lowest. The corresponding factor for the hot model map is 1.5.

The hot model map shows systematically higher fluxes than the modified cold model map, by a factor of from 1.3 to 2.0. Such differences are plausible. For example, the effect of ionization on the predicted flux depends on the shapes of the orbits whereby the scattering atoms reached the line of sight, and the effect of the solar line width depends on the radial component of gas orbital motion. At $T = 10^4$ K and $V_B = 20 \text{ km}\cdot\text{s}^{-1}$, a helium atom far from the Sun moving with transverse speed $V = (2kT/m)^{1/2} = 6 \text{ km}\cdot\text{s}^{-1}$ has an orbit vastly different from the one assumed by the modified cold model. Such thermally dispersed orbits are properly treated by the hot model but not by the modified cold model.

Crosswind Sky Map. In Figures 3 and 4 we show maps of 584 Å glow predicted by the modified cold model and hot model respectively, for an observer at a point on the Earth's orbit that is at 90° to the symmetry axis. As before, the distant gas bulk speed is $20 \text{ km}\cdot\text{s}^{-1}$ and the temperature is 10^4 K. The predictions are symmetric about a great circle containing

the antisolar point and the direction of gas motion, but the rectangular coordinates used in the figures obscure the symmetry.

Both models predict a localized region of high flux between the downstream direction of gas motion and the Sun, as is expected from the focusing of the gas orbits. However, as in the downstream case, the modified cold model predicts a markedly sharper region of maximum intensity than does the hot model. The predictions of the two models agree within fifteen per cent at the point of maximum intensity, but as the line of sight moves away from that point they diverge. At the north and south celestial poles, and in the direction from which the gas approaches, the hot model predicts about three times as much flux as does the modified cold model.

The Effect of Temperature. In order to investigate the effect of temperature on the predictions of the two models, we restricted the line of sight to directions pointing approximately radially outward from the Sun. We considered observers located at five points on the Earth's orbit: as close to the upwind and downwind symmetry axes as possible, at the crosswind position discussed above, and at approximately 135° and 160° from the upwind symmetry axis. With the LOS pointing approximately outward from the Sun from each observer position, we evaluated the model predictions while varying T from 625 to 80,000 K. We fixed V_B at $20 \text{ km}\cdot\text{s}^{-1}$ and set all other parameters to the values discussed above. We show the results of these calculations in Figure 5 for the modified cold model and in Figure 6 for the hot model.

The features of the modified cold model calculations are by now well understood. Temperature affects its predictions only in a region close to the downstream symmetry axis, whose exact size increases with T in the manner given by paraboloidally interpolating to the density given by Blum, Pfleiderer

and Wulf-Mathies (1975) equation (A17). The downstream LOS always lies within this region, hence the corresponding predictions vary with temperature. The high flux at low T indicates sharp focusing. The region where temperature variations occur does not expand to include the 160 degree LOS until T is between 10^4 and 2×10^4 K: thus predictions at 160 degrees are constant for lower temperatures. All other lines of sight never penetrate the temperature-sensitive region, hence the model predictions remain constant as T changes.

In contrast, the hot model exhibits considerable variation of predictions with temperature for all lines of sight. Note that even as far as 90 degrees from the downwind direction, varying T over the 1500 to 20,000 K range produces a fifty per cent change in predicted flux.

In the downwind direction at low temperature, the predictions of the two models differ substantially. We advise caution in ascribing great significance to this difference, because both models encounter unphysical infinities in the limit $T=0$. In the modified cold models, particle number density on the downwind axis diverges, and in the hot model, phase-space number density approaches a sum of Dirac delta functions. Inasmuch as our coding for both of these models was designed with temperatures above 3000 K in mind, it is possible that at substantially lower temperatures, the coding for one or both models produces inaccurate results.

IMPLICATIONS FOR RECENT DATA ANALYSES

After performing the tests and general calculations just discussed; we used the hot model to check some recently published 584 \AA observations which have previously been analyzed with the modified cold model. We first selected the satellite observations reported by Weller and Meier (1974). These authors presented data gathered during almost a year by a 584 \AA photometer whose LOS always maintained a constant 25-degree

angle with respect to the plane containing the Sun, the Earth, and the north celestial pole. Their instrument revolved rapidly about the normal to that plane, so that its LOS traced a cone of 130° apex angle. The cone in turn revolved at one revolution per year.

The greatest variations in the Weller and Meier data take place approximately at declination $+10^\circ$, as shown in Weller and Meier (1974), Figure 2. We selected values of Weller and Meier coordinate " α ", which describes the location and orientation of the cone, for which the 584 \AA isophotes in that Figure cross $\delta = +10^\circ$, and evaluated our hot model for the resulting observer positions and lines of sight. We used temperatures of 5000, 10,000 and 20,000 K, and set all other parameters as described above.

The results of our calculations are shown in Figure 7, in which the curve of short dashes is drawn through the data points taken from Weller and Meier and the curves labeled by temperature depict our hot-model predictions. In order to display the difference in shape of the curves clearly, we have multiplied each of our curves by a scale factor, to produce the same maximum intensity as the Weller and Meier data. This multiplication simply corresponds to an adjustment of the overall linear factors n_{∞} and F_{\odot} in the hot model.

Although each calculated curve might be said to have the same general shape as the Weller-Meier data curve, there are two systematic differences between theory and observations. First, the shapes of the curves are distinctly different near the region of maximum flux. The data resemble a Gaussian, but the calculated curves are more nearly triangular, with pointed tips and substantially broader bases. Second, none of the calculated curves display as high a ratio of maximum to minimum flux as do the data. We therefore are reluctant to state that the hot model fits that we have

obtained favor a specific temperature. Weller and Meier used the modified cold model to obtain a range of good fits between 5000 and 20,000 K, with the same values for the speed and direction of gas motion that we have used.

We conjectured that our calculations might have been done with too high a value of the ionization rate β_0 . If the selected value of $6.8 \times 10^{-8} \text{ s}^{-1}$ were greater than that actually present, then the model would predict excessively low helium number densities near the downwind symmetry axis, and consequently low flux levels. However, a few calculations (not shown) made with $\beta_0 = 0$ raised the ratio of maximum to minimum flux only half way to that observed by Weller and Meier,

Schmidtke (1976) has recently reported variations of the solar 584 \AA flux F_0 of as much as 30 per cent on a time scale of days to months. If F_0 had been 30 per cent higher for the $\alpha = 80^\circ$ data than for the $\alpha = 260^\circ$ data, then the theory and observations would be in better agreement. Unfortunately, Schmidtke's data do not include the time period in late 1972 when the Weller and Meier instrument was observing the region of high 584 \AA flux, so that no simple adjustment for varying F_0 is possible.

We have not determined what variations of other model parameters, such as the bulk speed and direction of motion of the distant gas, will produce a best fit of the hot model to the Weller and Meier observations. To do so would require a much more extensive analysis, using all of the Weller-Meier data instead of the small subset that we have chosen here. But our calculations clearly demonstrate that the hot and modified cold models can give substantially different results when used to analyze helium 584 \AA data. The differences between the models are therefore of considerable practical importance for the derivation of ISM parameters from observations.

Freeman et al. (1976a,b) used a 584 Å photometer equipped with a helium gas resonant absorption cell to study radiation scattered from $\alpha = 50^\circ$, $\delta = 39^\circ$. In their analysis, they used the ratio ϵ_0 of cell-full to cell-empty flux as a parameter for model fitting, and thereby reached conclusions independent of the exact values of n_∞ and F_0 . They obtained a lower limit, at a 95 per cent confidence level, of 10-15 km·s⁻¹ on the distant gas bulk speed V_b . We have used the hot model in an attempt to fit their data, with $T = 5000, 10,000$ and $20,000$ K and $V_B = 5, 10, 15, 20, 30,$ and 40 km·s⁻¹. All other parameters were set at the values discussed above. In Figure 8 we show how the hot model calculations fit the data of Freeman et al.. The horizontal dashed line is the observed value of ϵ_0 , and the shaded area depicts two standard deviation limits thereon. The curves labeled by temperature are the model predictions, which vary by up to 30 per cent over the range 5000-20,000 K. The lower limit on V_B indicated by the hot model, at a 95 per cent confidence level, is 17-20 km·s⁻¹, which is in better agreement with the recent results of Adams and Frisch (1977) and Bertaux et al., (1976) than was the limit derived using the modified cold model.

CONCLUSIONS

Figures 1-4 demonstrate that when the modified cold model and the hot model predictions for helium atoms are evaluated for physical parameters in the range presently believed correct, the hot model predicts broader intensity maxima and smaller total variations in flux level than does the modified cold model. The shapes of the intensity maxima are sufficiently complicated that the difference in shape is difficult to quantify, but the calculations presented here indicate that the patterns of 584 Å glow predicted by the two models are markedly different within

60 to 90° away from the projection of the downwind symmetry axis on the celestial sphere. We conclude that the modified cold model should not be used to analyze observations of this region.

Figures 3 and 4 indicate that at greater distances from the downwind axis, the shapes and spacings of the isophotes predicted by the two models are more similar, although the hot model predicts several times as much flux as the modified cold model. The modified cold model may possibly be of use for interpreting observations of this part of the sky, provided the analysis used depends only on the relative intensities of flux observed from different points. Future observers of 584 Å helium glow should address the question of model validity more specifically.

Figures 5 and 6 demonstrate that the hot model predicts substantial variations of observed flux with temperature, on lines of sight for which the modified cold model predicts no variation at all. Furthermore, even when the modified cold model does predict a variation of flux with temperature, the hot model predicts variations of a different kind. The use of the modified cold model to determine the precise temperature of the local ISM therefore appears invalid.

The conclusions drawn by previous observers of 584 Å flux who have used the modified cold model to interpret their data must be reassessed. The hot model does not reproduce the fit that Weller and Meier (1974) obtained using the modified cold model. We suggest that further study is in order, to determine the cause of the discrepancy and the actual values of the ISM parameters that the data imply. Point-by-point calculations of the particle number densities and velocity dispersions predicted by the two models would be useful in this context. When the hot model is used to analyze the data of Freeman et al. (1976) the derived lower limit to gas bulk speed is slightly nearer to the values of V_b obtained by other means than was the case with the modified cold model.

The theoretical question of the behavior of the local ISM is far from closed. Both the modified cold model and the hot model derive from two assumptions. First, the flow of the ISM through the solar system is assumed to be collisionless, so that each atom proceeds along a hyperbolic orbit determined by celestial mechanics. Second, the nearby ISM is assumed sufficiently tenuous that only singly-scattered photons will reach the observer. Wallis (1973, 1974, 1975) has questioned both of these assumptions. Further analytic and numerical study of their validity may be necessary before experimenters can have complete confidence in the interpretation of 584 Å data.

ACKNOWLEDGMENTS

This work was supported by NASA contract NAS9-13807. We thank Stuart Bowyer and Robert R. Meier for useful discussions. We thank a referee for several helpful comments..

REFERENCES

- Adams, T. F., and Frisch, P. C., 1977, *Astrophys. J.*, 212, 300.
- Banks, P. M., and Kockarts, G., 1973, *Aeronomy, Part A.*, Academic Press, New York and London, p. 157.
- Bertaux, J. L., Blamont, J. E., Tabarié, N., Kurt, W. G., Bourgin, M. C., Smirnov, A. S., and Dementeva, N. N., 1976, *Astron. Astrophys.*, 46, 19.
- Blum, P. W., Pfleiderer, J., and Wulf-Mathies, C., 1975, *Planet. Space Sci.*, 23, 93.
- Bowyer, S., Freeman, J., Paresce, F., and Lampton, M., 1977, *Applied Opt.*, 16, 756.
- Danby, J. M. A., and Camm, G. L., 1957, *Mon. Not. R. Ast. Soc.*, 117, 50.
- Delaboudiniere, J. P., and Crifo, J. F., 1975, paper presented at COSPAR meeting XVIII, Varna, Bulgaria, 1975 June 2.
- Doschek, G. A., Behring, W. E., and Feldman, U., 1974, *Astrophys. J.* (Letters), 190, L141.
- Fahr, H. J., 1974, *Space Sci. Rev.*, 15, 483.
- Fahr, H. J., Crifo, J. F., Wulf-Mathies, C., and Seidl, P., 1977, *Astron. Astrophys.*, 58, L21.
- Feldman, W. F., Goldstein, D., and Sherb, F., 1972, *J. Geophys. Res.*, 77, 5389.
- Freeman, J., Bowyer, S., Paresce, F., and Lampton, M., 1976b, *Rev. Sci. Instrum.*, 47, 277.
- Freeman, J., Paresce, F., Bowyer, S., and Lampton, M., 1976a, *Astrophys. J.*, 208.
- Meier, R. R., 1977, *Astron. Astrophys.*, 55, 211.

Milkey, R. W., Heasley, J. N., and Beebe, H. A., 1973, *Astrophys. J.*, 186,
1043.

Paresce, F., Bowyer, S., and Kumar, S., 1973, *Astrophys. J. (Letters)*,
183, L87.

_____, 1974, *Astrophys. J.*, 187, 633.

Schmidtke, G., 1976, *Geophys. Res. Letters*, 10, 573.

Wallis, M. K., 1973, *Astrophys. & Space Sci.*, 20, 3.

_____, 1974, *Mon. Not. R. Astr. Soc.*, 167, 103.

_____, 1975, *Planet. Space Sci.*, 23, 419.

Weller, C. S., and Meier, R. R., 1974, *Astrophys. J.*, 193, 471.

FIGURE CAPTIONS

Figure 1: Downwind Map-Modified Cold Model

Modified cold model predictions of interplanetary 584 \AA glow seen from the downwind side of the Earth's orbit, for $V_B = 20 \text{ km s}^{-1}$, $T = 10^4 \text{ K}$. Isophotes in rayleighs interpolated between calculated predictions. The map is symmetric about $\alpha = 72^\circ$. Direction toward which gas flows indicated by \ominus .

Figure 2: Downwind Map-Hot Model

Hot model predictions of interplanetary 584 \AA glow seen from the downwind side of the Earth's orbit, for $V_B = 20 \text{ km s}^{-1}$, $T = 10^4 \text{ K}$. Isophotes in rayleighs interpolated between calculated predictions. The map is symmetric about $\alpha = 72^\circ$. Direction toward which gas flows indicated by \ominus .

Figure 3: Crosswind Map-Modified Cold Model

Modified cold model predictions of interplanetary 584 \AA glow seen from the Earth's orbit midway between upwind and downwind symmetry axes, for $V_B = 20 \text{ km s}^{-1}$, $T = 10^4 \text{ K}$. Isophotes in rayleighs interpolated between calculated predictions. Gas flows from direction indicated by \oplus , toward direction indicated by \ominus . Antisolar point indicated by \otimes .

Figure 4: Crosswind Map-Hot Model

Hot model predictions of interplanetary 584 \AA glow seen from the Earth's orbit midway between upwind and downwind symmetry axes, for $V_B = 20 \text{ km s}^{-1}$, $T = 10^4 \text{ K}$. Isophotes in rayleighs interpolated between calculated predictions. Gas flows from direction indicated by \oplus , toward direction indicated by \ominus . Antisolar point indicated by \otimes .

Figure 5: Effect of Temperature-Modified Cold Model

Modified cold model predictions of interplanetary 584 Å glow seen from various points on the Earth's orbit, looking radially outward from the Sun, as a function of temperature, for $V_B = 20 \text{ km s}^{-1}$. Curves interpolated between calculated predictions. Curve labels are angles between line of sight and upwind symmetry axis.

Figure 6: Effect of Temperature-Hot Model

Hot model predictions of interplanetary 584 Å glow seen from various points on the Earth's orbit, looking radially outward from the Sun, as a function of temperature, for $V_B = 20 \text{ km s}^{-1}$. Curves interpolated between calculated predictions. Curve labels are angles between line of sight and upwind symmetry axis.

Figure 7: Weller-Meier Data Fit

Use of hot model to fit data of Weller and Meier (1974). Line of short dashes: interpolation between Weller and Meier data points. Other lines: hot model predictions for the stated temperatures, scaled to the same maximum flux observed by Weller and Meier. The coordinate α describes the Weller and Meier viewing geometry.

Figure 8: Freeman et al. Data Fit

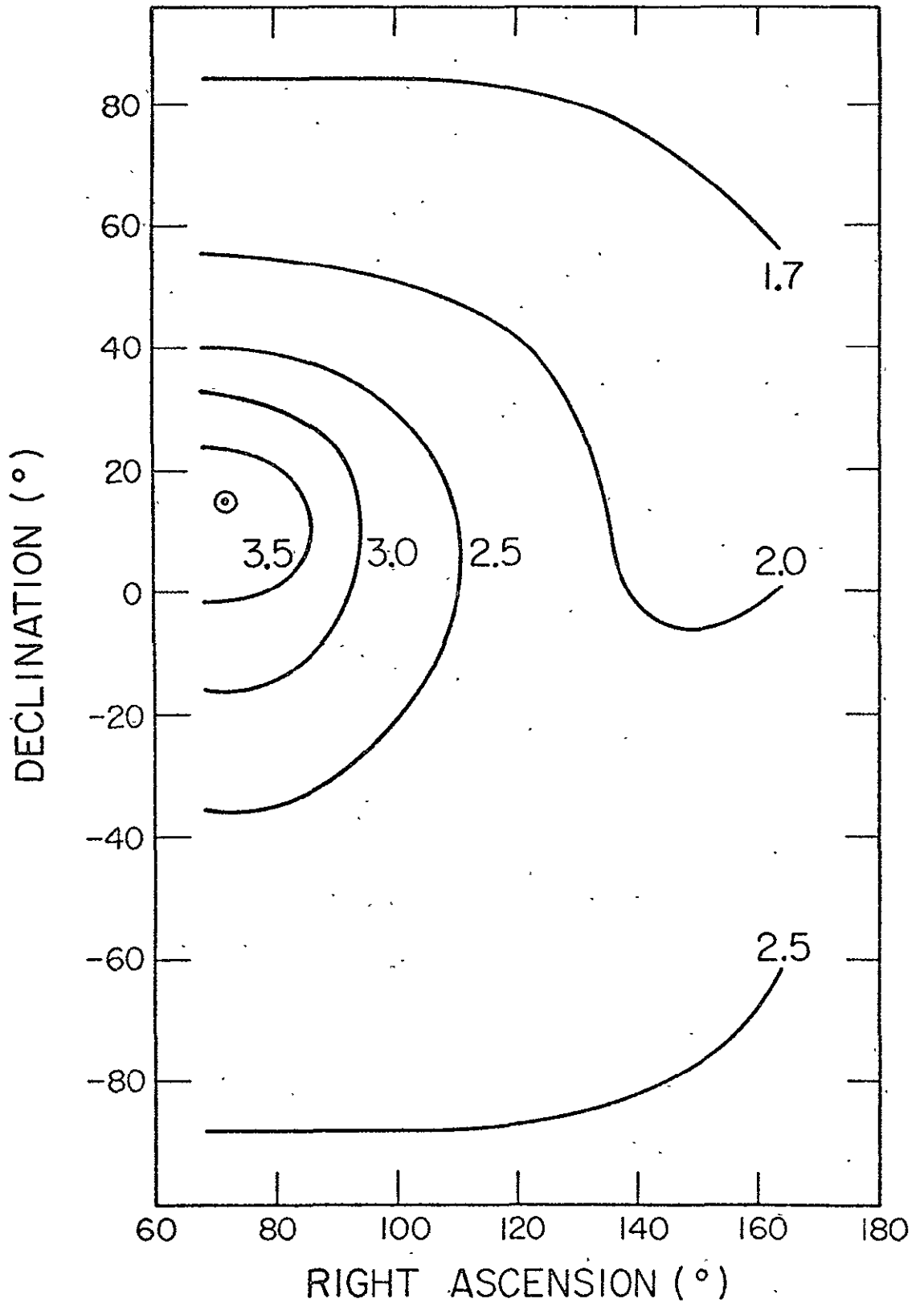
Use of hot model to fit data of Freeman et al. (1976a). Dashed line: observed ratio of cell-full to cell-empty flux. Shaded area: two standard deviation limits on ratio. Labeled curves: hot model predictions for the stated temperatures, as a function of distant gas bulk speed.

J. Freeman

F. Paresce

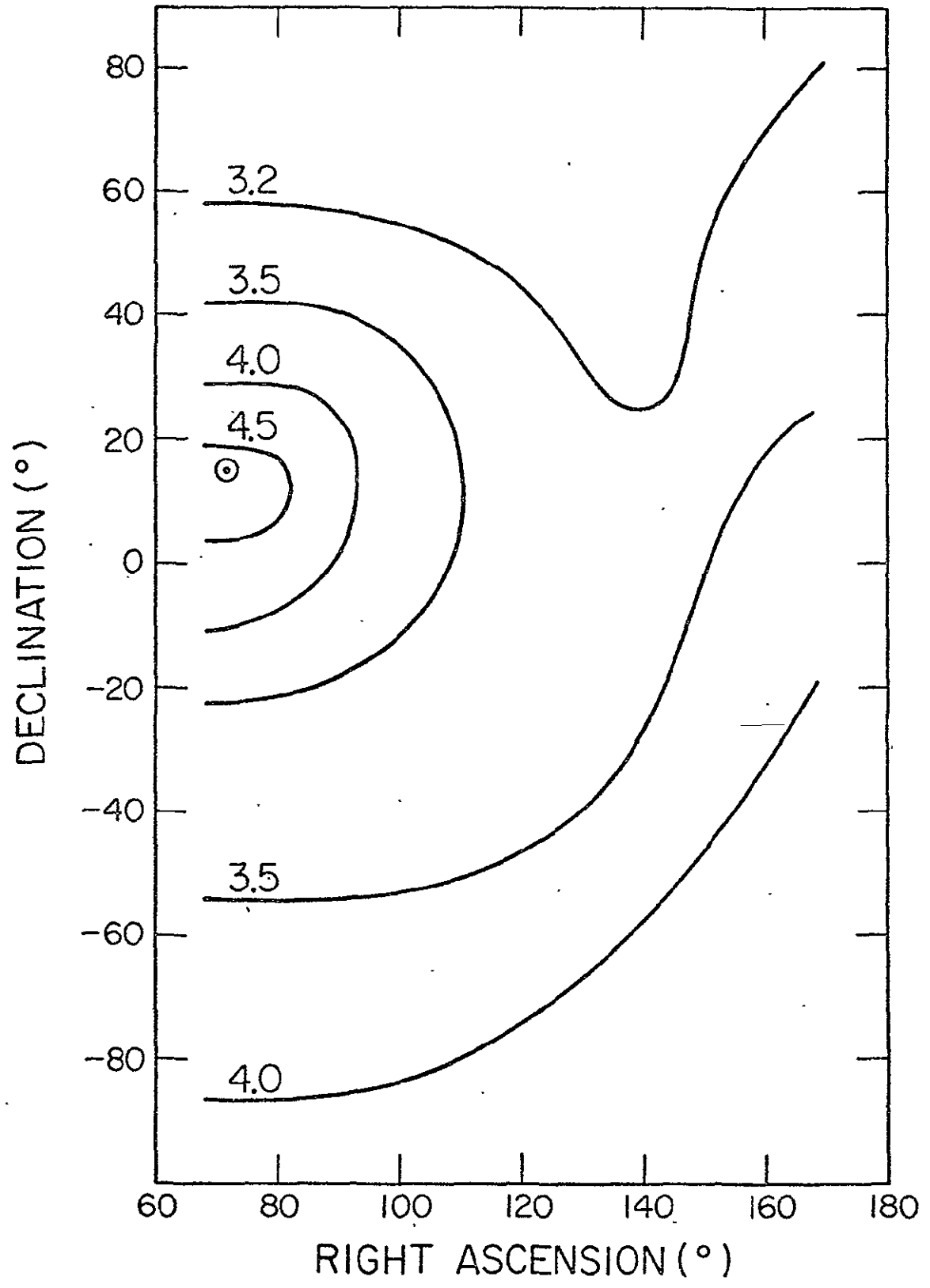
Space Sciences Laboratory
University of California
Berkeley, CA 94720

FIGURE 1



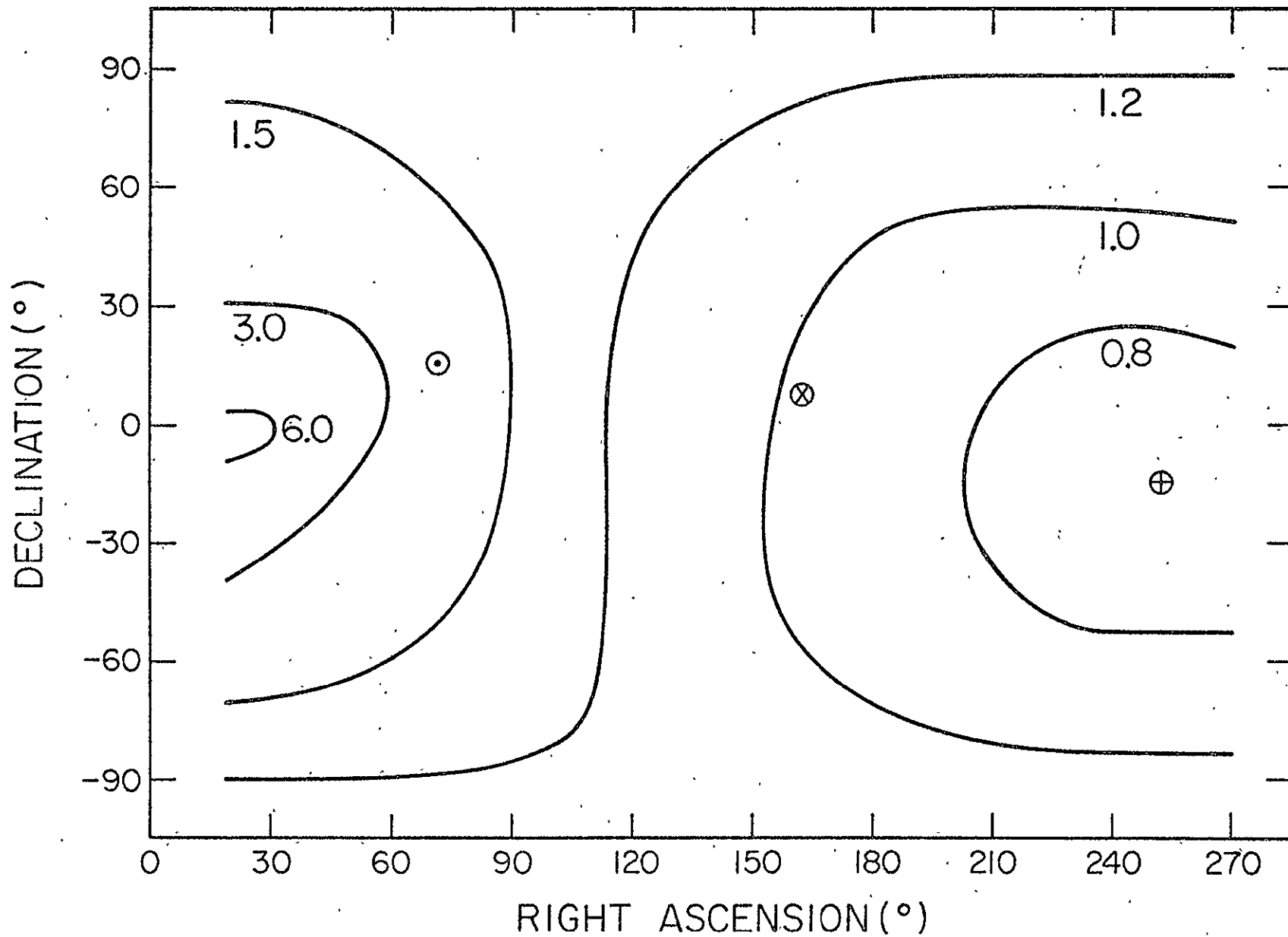
DOWNWIND MAP
MODIFIED COLD MODEL

FIGURE 2



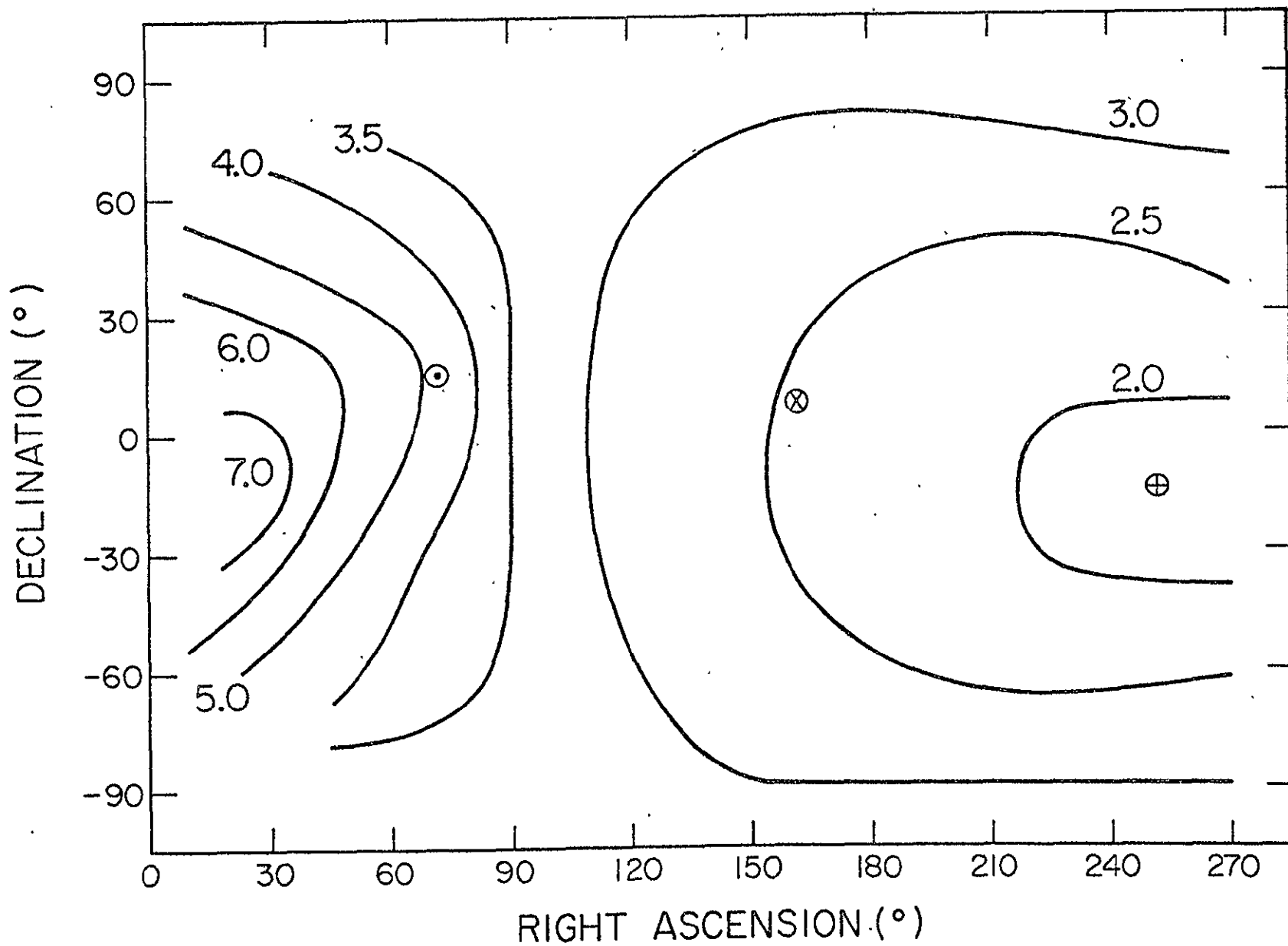
DOWNWIND MAP-HOT MODEL

0.2

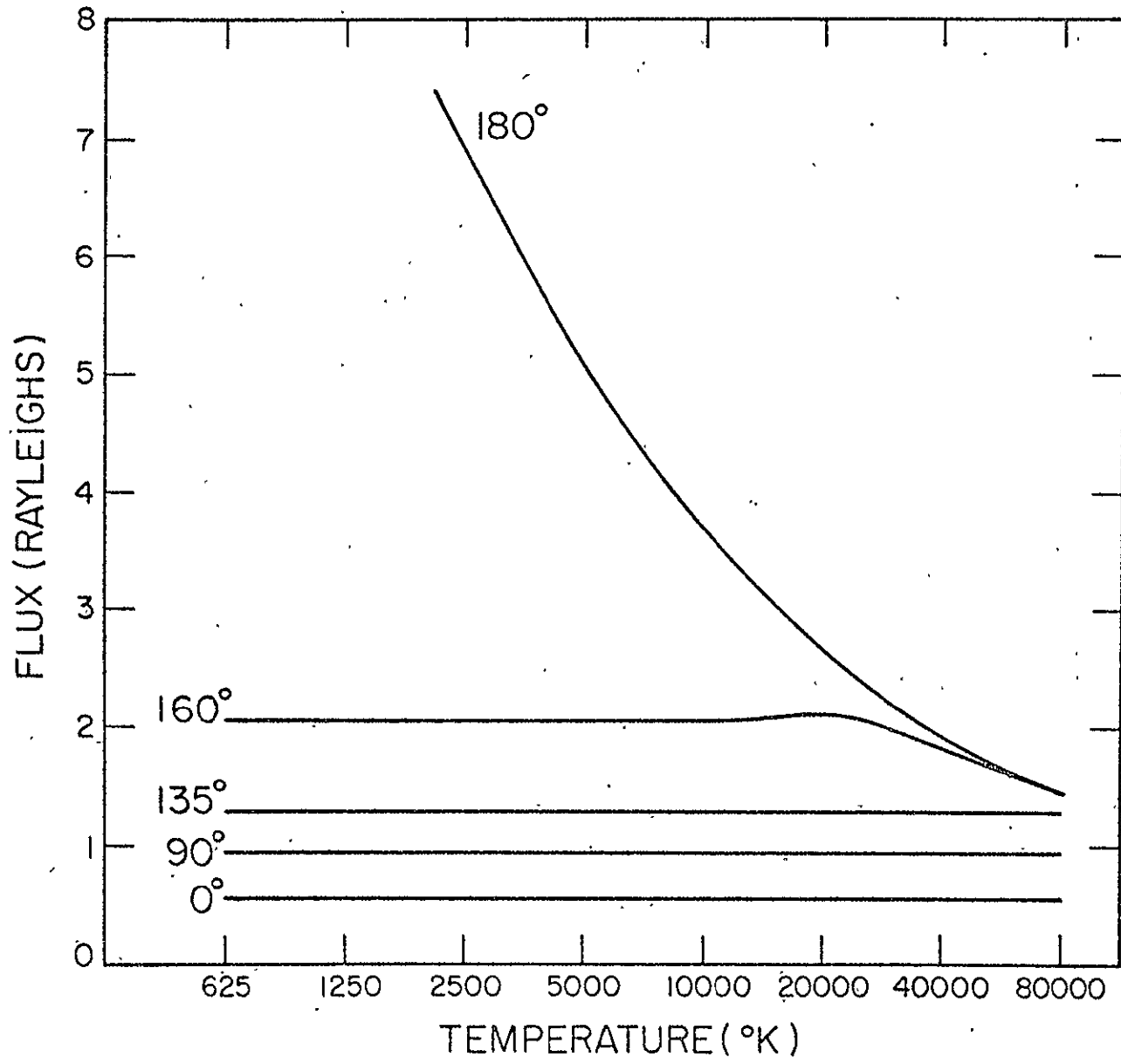


CROSSWIND MAP—MODIFIED COLD MODEL

FIGURE 3

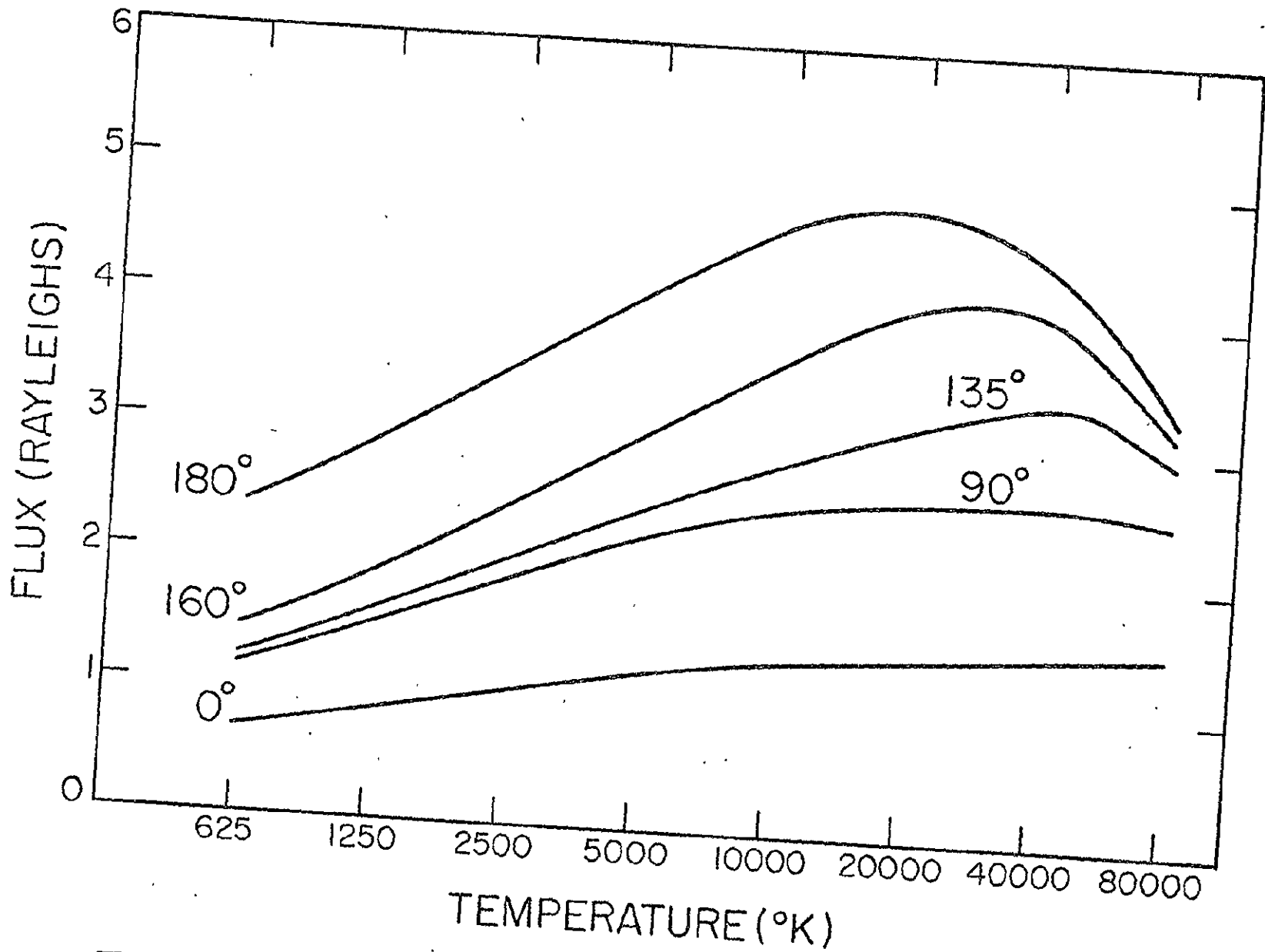


CROSSWIND MAP - HOT MODEL



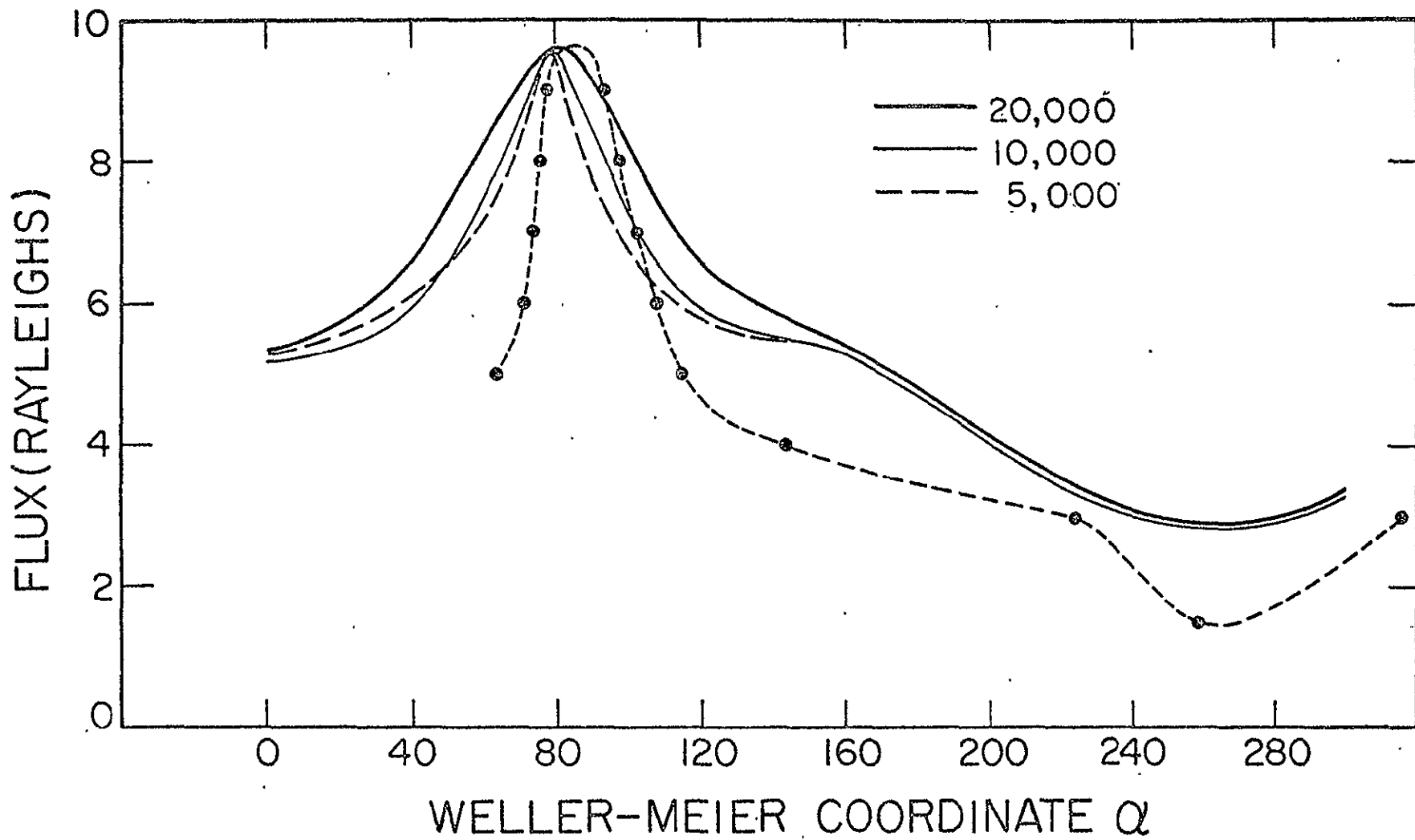
EFFECT OF TEMPERATURE
MODIFIED COLD MODEL

FIGURE 5



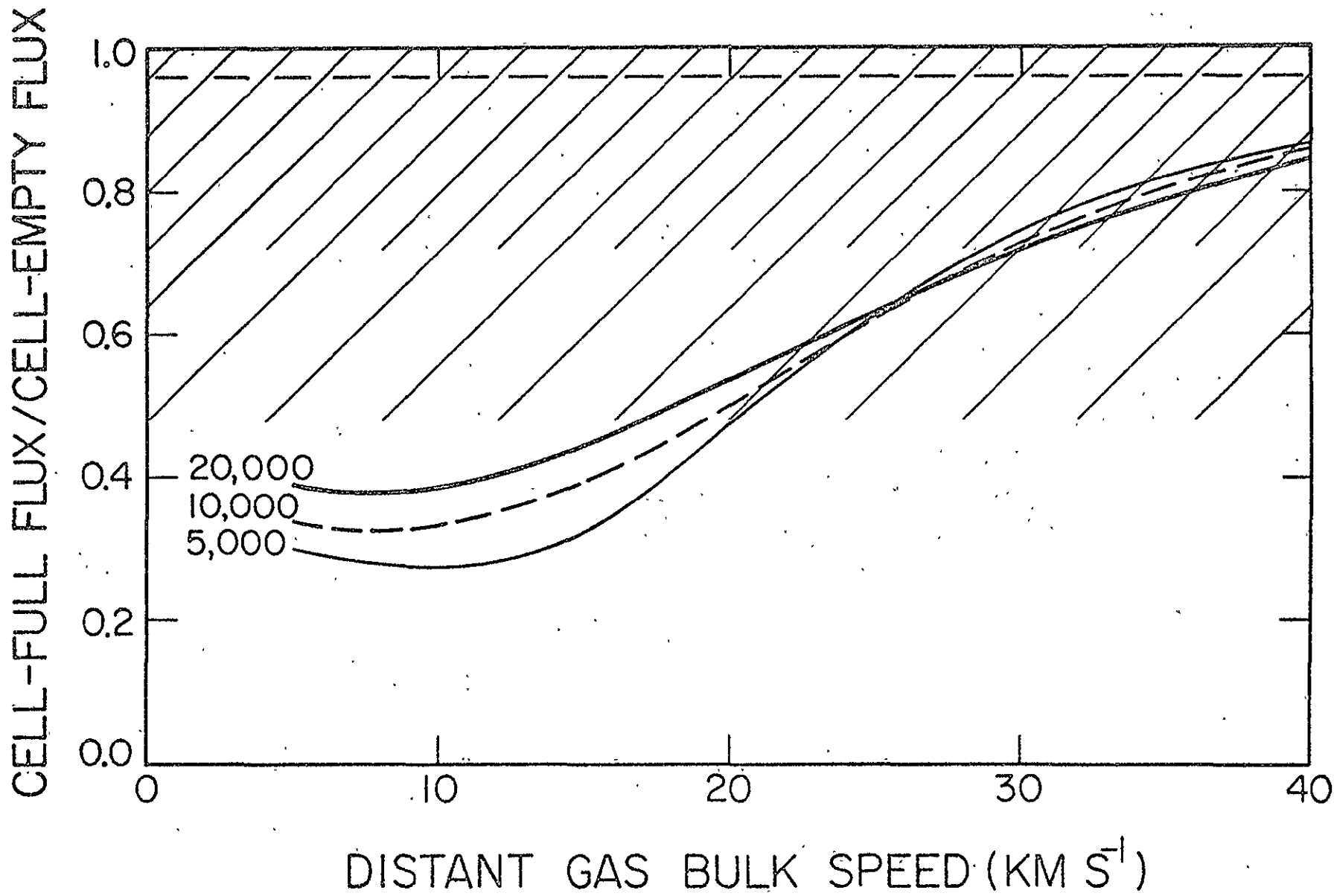
EFFECT OF TEMPERATURE — HOT MODEL

FIGURE 6



WELLER-MEIER DATA FIT

FIGURE 7



FREEMAN ET AL. DATA FIT